OVERVIEW OF FUSION BLANKET R&D IN THE US OVER THE LAST DECADE

M. A. ABDOU*, N. B. MORLEY, A. Y. YING, S. SMOLENTSEV and P. CALDERONI
Mechanical & Aerospace Engineering Department, 44-114 Engineering IV, 420 Westwood Plaza
University of California, Los Angeles CA 90095-1597, USA
*Corresponding author. E-mail : abdou@fusion.ucla.edu

Received September 5, 2005

We review here research and development progress achieved in US Plasma Chamber technology roughly over the last decade. In particular, we focus on two major programs carried out in the US: the APEX project (1998-2003) and the US ITER TBM activities (2003-present). The APEX project grew out of the US fusion program emphasis in the late 1990s on more fundamental science and innovation. APEX was commissioned to investigate novel technology concepts for achieving high power density and high temperature reactor coolants. In particular, the idea of liquid walls and the related research is described here, with some detailed examples of liquid metal and molten salt magnetohydrodynamic and free surface effects on flow control and heat transfer. The ongoing US ITER Test Blanket Module (TBM) program is also described, where the current first wall / blanket concepts being considered are the dual coolant lead lithium concept and the solid breeder helium cooled concepts, both using ferritic steel structures. The research described for these concepts includes both thermofluid MHD issues for the liquid metal coolant in the DCLL, and thermomechanical issues for ceramic breeder packed pebble beds in the solid breeder concept. Finally, future directions for ongoing research in these areas are described.

KEYWORDS : Liquid Walls, Magnetohydrodynamics, Free Surface Flow, Packed Bed Thermomechanics, APEX, ITER Test Blanket Modules

1. INTRODUCTION

Developing a vision for an economically competitive fusion energy system remains the grand challenge for fusion researchers. Meeting this challenge requires advances in plasma physics and in fusion technology, a key element of which is Fusion Power Technology (FPT), also called Fusion Nuclear Technology (FNT). FPT is concerned with all reactor components in the immediate exterior of the plasma, commonly called "in-vessel systems", which include first wall, divertor, blanket, and the vacuum boundary as shown in Fig. 1. The functional requirements of FPT are to:

- provide a VACUUM environment
- EXHAUST plasma burn products
- EXTRACT POWER from plasma particles and radiation (surface heat loads)
- EXTRACT POWER from energy deposition of neutrons and secondary gamma rays
- BREED TRITIUM at the rate required to satisfy tritium self sufficiency
- provide RADIATION SHIELDING for other sensitive components (*e.g.*, superconducting magnets) and the environment

FPT components must perform these functions reliably in steady-state in the harsh fusion environment without disturbing the plasma and while also allowing for plasma heating, fueling, and stability control, which often requires large penetrations through the breeding blankets and first wall, and highly conducting coils and shells close to the plasma.

FPT has many engineering science and technology development issues whose resolution, together with the development of simple plasma confinement configurations, will be the most important element in determining the economic competitiveness of fusion energy systems. In the present paper, we review the R&D programs and progress in the US over the timescale encompassing the last decade with particular focus on critical engineering science topics related to the thermofluid and thermomechanical feasibility of the blanket systems.

2. SUMMARY OF TECHNICAL PROGRAMS AND ISSUES

Fusion Power Technology development over the preceding decade has progressed through several important transformations. In the early to middle 1990s, the US was heavily involved in the Engineering Design Activity (EDA)

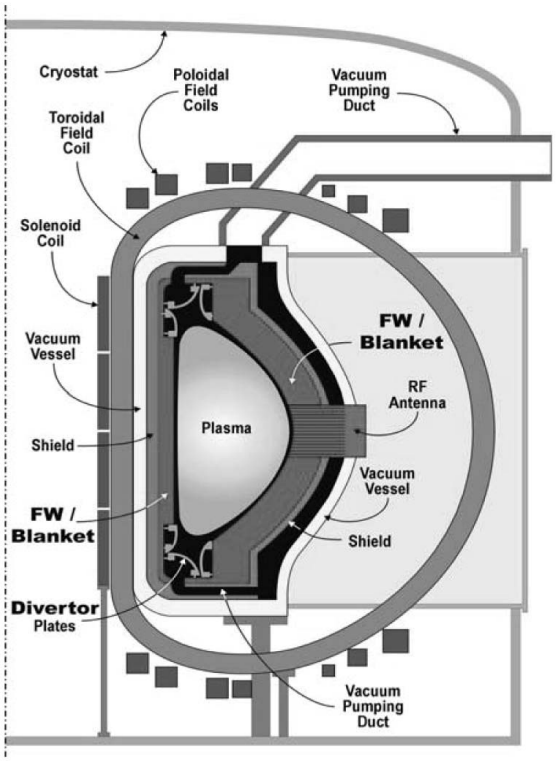

Fig. 1. Fusion Reactor Cross-Section Showing Fusion Power Technology Components

for ITER as well as programs in the definition and preparation of Test Blanket Modules (TBMs) for ITER [1], and in the definition of a Component Test Facility (CTF) [2] known at that time as the Volumetric Neutron Source (VNS) for testing of reactor relevant first wall and blanket technologies to meaningful fluence levels. In terms of blanket technologies of interest, the US was pursuing the development of self-cooled lithium with vanadium structure and insulator coatings, and helium-cooled ceramic breeder blankets with beryllium neutron multiplier and ferritic steel structure.

2.1 Critical Fusion Power Technology Issues

Critical FPT issues related to blanket and first wall systems were certainly well known for some time, but over the past decade have come into sharper focus. In particular, the following list summarizes the most important FPT critical issues, a few of which we will expand upon in subsequent paragraphs and sections of the paper.

1. Tritium Supply & Tritium Self-Sufficiency
2. High Power Density leading to compact devices
3. High Temperature leading to high efficiency
4. MHD for Liquid Breeders / Coolants
5. Tritium Control (Permeation)
6. Reliability / Availability
7. Testing in Fusion Facilities

2.1 Tritium Supply and Tritium Self-Sufficiency

In particular, the availability of tritium supply has been a central issue for the development of fusion energy. D-T plasmas consume huge amounts of tritium, unprecedented in the history of mankind. This tritium cannot be provided for long from non-fusion tritium production sources. Tritium consumption in D-T devices is 55.8 kg per 1000 MW of fusion power per year. In contrast, the tritium supply available for fusion accumulated over 40 years of CANDU reactors operation will peak at 27 kg in the year 2027 and, if not consumed sooner, will decay at a rate of 5.47% per year. It must be also clearly recognized that all D-T experimental devices, and, of course, the DEMO and power plants, will have to breed their own tritium. This puts a premium on integrated testing of tritium breeding blanket concepts in ITER. Without a successful TBM in ITER, the world will not have an adequate tritium supply for fusion energy development – an ironic consequence considering the fundamental promise of fusion as an "inexhaustible energy source". The D-T cycle is the basis of the current world plasma physics and technology program. As for tritium self sufficiency requirements, it should be recognized that there is only a "window" of physics and technology parameters in which the D-T cycle is feasible. Determination of this "window" is a critical need because if the D-T cycle is not feasible, the plasma physics and technology research would be very different.

To analyze the issue of fuel self-sufficiency, it is necessary to account for the performance of the blanket in terms of generating tritium on one side, and the necessary amount of tritium that needs to be circulated and stored in the facility on the other. The first is addressed by calculating the *achievable* Tritium Breeding Ratio of a specific power plant concept, and is a function of technology, material and physics design and operating conditions. The concepts and materials used in chamber components (blanket, divertor, *etc.*) have significant impact on the achievable TBR, as well as on the confinement scheme, primarily due to the impact on breeding blanket coverage and possible limitations on blanket thickness and the presence of conducting shells and coils in the breeding region. Calculation of the achievable TBR should be based on detailed three-dimensional (3-D) neutronic analysis that accounts for all design details of the system. The US community has been actively involved in the initial analysis of the performance of proposed chamber and blanket systems design in terms of achievable TBR. A summary of these efforts is given in [3]. Other examples of TBR performance evaluation of specific blanket systems can be found in [4-10].

The second part of the fuel self-sufficiency analysis is addressed by calculating the *required* Tritium Breeding Ratio. The required TBR should exceed unity by a margin sufficient to: (a) compensate for losses (inventory trapped in components for example) and radioactive decay of tritium during the period between production and use, (b) supply inventory for startup of other reactors, and (c)

provide a "holdup" or "reserve" storage inventory necessary for continued reactor operation under certain conditions. An example of a need for a storage inventory is that kept in reserve to keep the power plant operating while there is a failure in a tritium processing line, such as the plasma exhaust line. To accurately determine the required TBR, one has to consider the "dynamics" of the entire fuel cycle for the D-T plant that involves many subsystems. Because of tritium radioactive decay, it is essential to accurately calculate the time-dependent tritium inventories and flow rates throughout the system. The main subsystems of the power plant with significant tritium inventories are plasma exhaust and vacuum pumping, first wall (FW), blanket, plasma-facing components (PFC), fuel clean-up, isotope separation, fuel management, storage, and fueling. Simulation of this cycle, including the dynamic behavior of tritium inventories and flow rates, has been an important part of the US Fusion Technology research effort. Abdou [11] first developed in 1986 a detailed analytic model to both describe various tritium processes and to quantify the characteristic parameters of the various elements of the tritium fuel cycle as a tool for evaluating the required TBR. The work was expanded in 1999 [12] to account for the details of the operation of key sub-systems of the fuel cycle, such as the Isotope Separation System and the cryogenic pumps of the plasma exhaust line. The analysis of the dependence of the required TBR on many design and operational parameters of a fusion energy system is also summarized in [3].

The objective of the fuel cycle analysis is to identify a "window" of parameters that can lead to satisfying the tritium self-sufficiency condition, which are those for which the achievable TBR is higher than the required TBR. Figure 2 is an example of such a parameters "window". As discussed in [3], the achievable TBR for fusion energy systems is likely to be less than about 1.15, which is represented by the shaded area in the graph. The required TBR is calculated in this example as a function of two of the most important parameters: the fractional fuel burn-up (the fraction of the rate at which the fuel that is used in D-T reactions versus the total rate of fuel injected in the system) and the doubling time (the time required to store the necessary start-up inventory for a new power plant). For a list of the other operational conditions assumed in the calculations refer to [3,12].

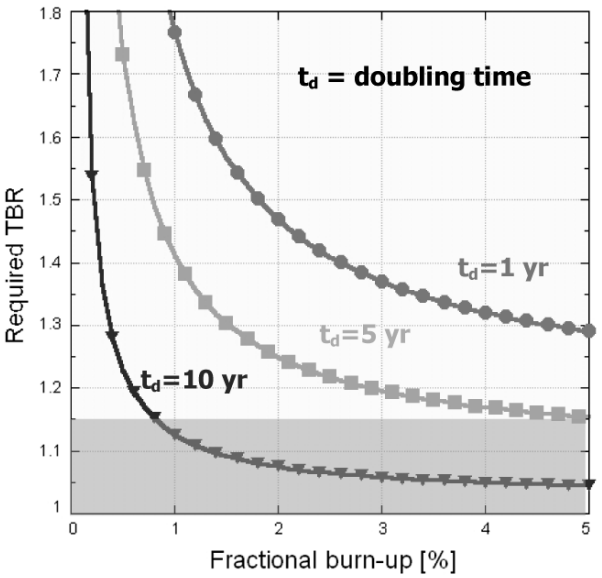

Fig. 2. Example of Parametric Dependence of "Window" for Tritium Self-Sufficiency

2.2 APEX Program and High Power Density

In the late 1990s, the US decided to discontinue participation in ITER and restructure the US program with an emphasis on innovation and fundamental scientific understanding. The APEX (Advanced Power Extraction) program [13, 14], initiated in the US in early 1998, was centered on exploring *novel* concepts for fusion technology that could substantially improve the attractiveness of fusion energy systems. The chamber technology performance goals in APEX included: (1) high power density capability with neutron wall load > 10 MW/m^2 and surface heat flux > 2 MW/m^2, (2) high temperature leading to high power conversion efficiency (>40%), (3) high availability, and (4) simple technological and material constraints.

To realize these goals, two classes of innovative concepts emerged that offer great promise: liquid walls and high temperature solid walls. The liquid wall concept seeks to eliminate the solid "bare" first wall by utilizing flowing liquids facing the plasma. In the course of the APEX study, this liquid wall idea resulted in a number of concepts that vary in the: (a) working liquid, (b) type of restraining force used to control the liquid, and (c) desired hydrodynamic flow configuration. The second class of concepts focused on ideas for extending the capabilities of solid first walls. The most promising concept, called EVOLVE [15], is based on the use of a high-temperature refractory alloy with an innovative cooling scheme that utilizes vaporization of lithium. Another concept utilizes advanced nanocomposite ferritic steel (AFS) as the structural material and molten salt FLiBe as the tritium breeder and coolant [16]. It should be noted that in addition to the APEX effort, R&D on insulator coatings and vanadium for the Li/V blanket system and on solid breeder thermomechanics for solid breeder based blanket systems, as the respective critical issues for these concepts, continued during this period as well.

2.2.1 Types of Liquid Walls

The most promising group of novel concepts for APEX was the flowing liquid wall (Fig. 3). Liquid wall concepts vary from "thin liquid walls", where a thin layer of liquid (~ 1-2 cm) flows on the plasma side of the first wall with

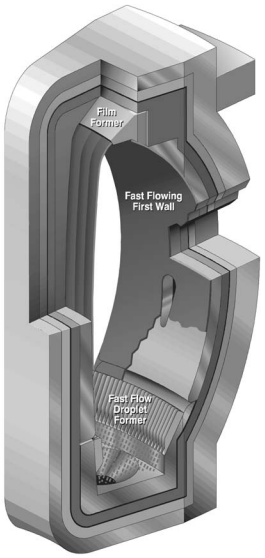

Fig. 3. Illustration of the Liquid Wall Idea. Liquid (liquid metal or molten salt) Injected at the Top of the Chamber Flows Down Along the Solid Structural wall Under the Gravity, Inertia and Centrifugal Forces. The Liquid Absorbs Surface Heat Flux and Neutron Volumetric Heating. The Liquid is Extracted from the Chamber at the Bottom

a conventional blanket behind, to "thick liquid walls," where a thick layer (> 40 cm) removes both the surface and volumetric heat and provides adequate breeding at the same time. It was shown in APEX that the thin wall concept, while serving only to remove the first wall surface heat load, has fewer feasibility issues related to the control of the hydrodynamic configuration when compared to the thick liquid wall.

Other variations of the liquid wall concept include the type of the "restraining force," which provides liquid adherence to the back wall via inertial, gravitational, centrifugal or even special electromagnetic effects. Correspondingly, there can be gravity-momentum driven (GMD), electromagnetically restrained (EMR), or liquid wall flows driven by the magnetic propulsion effect [17].

While all concepts in the liquid wall category share some common features, each concept has its own unique set of incentives and issues. All liquid wall concepts offer, however, many potential advantages that may be realized providing a good liquid wall design can be developed:

- High power density capability and improved disruption survivability by elimination of thermal stress and wall erosion as limiting factors;
- Improvements in plasma stability and confinement through particle pumping and close fitting electrical shell effects;
- Reduced volume of radioactive waste and radiation damage in structural materials by shielding solid reactor components;
- Potential for higher availability via increased lifetime and reduced failure rates and faster maintenance (design-dependent).

It is not clear that all of these advantages can be realized simultaneously in a single concept. However, the realization of only a subset of these advantages will result in remarkable progress toward the attractiveness of fusion energy systems.

The thin liquid wall concepts in the APEX study are called CLiFF (the Convective Liquid Flow First-Wall concept). The idea behind CLiFF is to eliminate the presence of a solid first wall facing the plasma. This goal is accomplished by means of a fast moving (~10 m/s), thin (~2 cm) liquid layer flowing on the first structural wall surface. This thin layer is a renewable surface immune to radiation damage and sputtering concerns, and largely eliminates thermal stresses and their associated problems in the first structural wall. The thin wall removes the surface heat flux, while most of the neutron absorption and tritium breeding occurs in the conventional blanket located behind the structural wall. The general CLiFF design is conceptually simple. A layer of liquid is injected near the top of the plasma chamber. The layer flows down the reactor walls without excessive thinning, and is removed in some fashion from the bottom of the chamber. The centrifugal acceleration in the liquid due to flow over the curved back wall of the plasma-shape-fitted structure provides an adhesion force that can be several times the typical acceleration of gravity. Another way to create the restraining force is to use the magnetic propulsion scheme (for liquid metals). In such configuration, the liquid metal is injected at the inboard of the reactor chamber and extracted at the outboard. The flow is driven by the electromagnetic propulsion effect, which appears due to MHD interaction between an applied electric current and the non-uniform toroidal magnetic field.

The majority of the work on the thin liquid wall concepts was carried out for the tokamak. Specifically, the ARIES-RS [18] geometry was utilized whenever possible, with modifications for the unique structures and high flow rates required for CLiFF. This means, however, that the ARIES-RS fusion power needs to be scaled-up to 4500 MW to give the 10 MW/m^2 peak neutron wall load and 2 MW/m^2 peak surface heat flux, which are the goals of the APEX study. Many related studies conceptually close to the basic CLiFF idea were also performed for the NSTX reactor [19]. One of the goals of these exploratory studies was to access different film flow schemes suitable for lithium divertor particle pumping and surface heat removal under complex magnetic fields.

The liquid wall concepts based on the idea of thick flow are even more attractive than the thin liquid wall concepts. The replacement of the first wall with a flowing thick liquid offers the potential advantages of high power density, high reliability and availability (due to simplicity and low failure rates), reduced volumes of radioactive waste, and increased structure lifetime. However, establishing a stable thick liquid wall configuration appears to be a more challenging goal in comparison with the thin flow. Design ideas for

Table 1. Typical Liquid Metal and Molten Salt Thermophysical Parameters

Properties	Units	FLiBe	Lithium
Composition	Mole %	66% LiF + 34% BeF2	100% Li
Melting Point	K	733	459
Operating Point	K	773	673
Density	kg/m^3	2036	490
Dynamic Viscosity	kg/m/s	0.015	4.02×10^{-4}
Kinematic Viscosity	m^2/s	7.37×10^{-6}	8.19×10^{-7}
Electrical Conductivity	S/m	155	3.19×10^{6}
Thermal Conductivity	W/m/K	1.06	50.4
Heat Capacity	J/kg/K	2380	4209
Surface Tension	N/m	0.2	0.366

establishing thick liquid walls were addressed for the tokamak (ARIES-RS), spherical torus (ST), and field reverse configuration (FRC) [20]. The second phase of APEX (beginning around 2000) had, however, narrowed the scope of liquid wall research to focus predominantly on thin first wall flows. Several thin wall designs have been undertaken that utilize Li, Sn, Sn-Li and two molten salts. Presented here are highlights from the design work, where we especially feature the FLiNaBe design in some detail as the most recent and complete [21]. The studies performed assumed top-bottom flow rather than the magnetic propulsion scheme due to the difficulty of introducing the working liquid at the inboard midplane.

2.2.2 Working Fluids and Associated Liquid Wall Designs

Candidate liquids for use as a liquid wall range from high conductivity, low Prandtl number liquid metals to low conductivity, high Prandtl number liquids such as molten salts. The hydrodynamics and heat transfer related characteristics and issues of high-conductivity, low Prandtl number liquid metals are considerably different from those of the low-conductivity, high Prandtl number molten salt flows. Flowing liquid metals may require the use of electrical insulators to overcome the MHD drag, while MHD effects caused by the interaction with the mean flow are less significant for the molten salt free surface flows. The effects on plasma stability and confinement are also different based on the electrical conductivity of the working liquid.

Several different *thin* liquid wall design studies were performed using different working liquids. The FLiBe and lithium designs had problems with limited windows for operating temperature. Excessive surface temperature (vaporization of fluorine) limited the FLiBe design, and poor thermal efficiency limited the lithium design. The limit in each case was the allowable impurity generation from the wall and this in turn set the restriction in the surface temperature of the fluid [22].

These conclusions led to the consideration of tin as the first wall stream with a separate PbLi blanket. The analysis of plasma surface interactions gave a fairly good operating temperature range with the surface temperature limit of tin being 810-840°C for the first wall and 1630°C for the divertor. However, predictions of complex 3D flows for the liquid metal systems were not available due to the difficulty of modeling the magnetohydrodynamic (MHD) effects that dominate the fluid flow for liquid metal systems in a magnetic fusion reactor. MHD calculations for lithium (and tin), with 1D and 2D models for the MHD forces and the assumption of an insulating wall, did show that fast thin layers would flow down and adhere to a concave substrate [23].

Finally, a design with the molten salt FLiNaBe as the working fluid was evaluated. FLiNaBe is a mixture of lithium, beryllium and sodium fluorides and, while similar to FLiBe, has a lower melting point (~300-315°C) [24]. This lower melting point extends the window of operating temperature enough that a workable design appears possible.

As suggested above, the MHD effect on free surface flows of liquid metals at this time was a big uncertainty and remains a feasibility issue for liquid walls. Significant research continues to be performed in an attempt to develop a predictive capability and experimental simulation of liquid wall flows. This work is described in more detail in Section 3. The consideration of molten salts as an alternative to liquid metals does not completely eliminate issues associated with MHD (see table 1 for a comparison of typical LM and molten salt thermo-physical properties). Molten salts have low electrical conductivity compared to LMs, but the electrical conductivity does not vanish and is in fact roughly 30x *greater* than typical seawater. MSs also have low thermal conductivity, on the order of water, and must rely on turbulent convective heat transfer to limit the peak surface temperature. This turbulence is potentially affected by the strong magnetic field, and the degree to which it might affect heat transfer is uncertain. The use

of MSs also has feasibility issues associated with the control of corrosion coming from the free fluorine and hydrogen-fluoride generated during breeding in a neutron field. A reducing agent (like Be) will be required to eliminate these corrosive breeding products before they can attack the structural walls. Detailed research in both these areas is continuing in the US as part of the JUPITER-II collaborative program with Japan [25].

2.2.3 Example: FLiNaBe Thin Liquid Wall Design

Figure 4 shows the flow streams and bulk temperatures for the final APEX design with FLiNaBe as described in detail in [21]. The inboard and outboard first wall streams flow from a set of nozzles at the top of the chamber that inject the liquid onto the front surfaces of the blanket modules. One set of nozzles feeds the inner first wall and another set feeds the outer first wall. The overlapping streams from the "self-shielding" nozzles prevent any line-of-sight from the plasma directly to a nozzle. The thickness of the first wall flow at midplane is 23 mm and the flow speed is 10 m/s. The FLiNaBe bulk temperature is 402ºC and rises to 420ºC at the bottom of the first wall. The maximum estimated surface temperature of the first liquid wall is 532ºC without accounting for the advantage of the wavy flow and 492ºC with waviness. Since we anticipate that some waviness will occur, we conclude that the maximum surface temperature will not exceed the allowable maximum surface temperature of 510ºC, and the first wall power handling is adequate.

Near the bottom of the plasma chamber, these first wall streams cover the inboard and outboard divertor as well. In the divertor, charged particles hitting the surface at the "strike point" produce a peaked heat load. The rise in surface temperature for the divertor stream is calculated to be about 135ºC; this, added to the bulk temperature of 420ºC leaving the first wall, gives a peak of about 555ºC. This is higher than the allowable temperature of 510ºC for the first wall, but is acceptable in the divertor where there is more shielding of impurities from the main plasma. The estimation of surface heat transfer of the turbulent

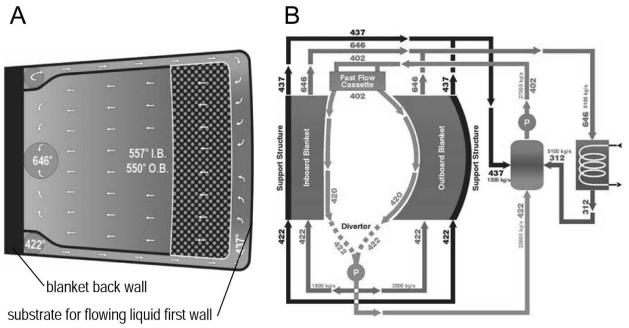

Fig. 4. FLiNaBe Liquid Wall Design. Cross-Section of Outboard Blanket Module (A) and Flow Streams and Bulk FLiNaBe Temperatures (B) are Shown

FLiBe flow was a key issue for APEX, and the experimental and modeling research performed in this area is described in more detail in Section 3 of this paper.

A conventional blanket is located behind the structural wall. The radial build of the inboard blanket is 544 mm; that of the outboard blanket is 644 mm. Both have a 5 mm front wall, 40 mm FLiNaBe plenum and 60 mm beryllium bed (57% packing density) to aid in breeding and in HF control. The walls are advanced ferritic steel. The main breeding region at the back of the blanket is 400 mm deep in the inner blanket and 500 mm deep in the outer blanket. The blanket collects about 80% of the heat produced by the reactor. The FLiNaBe stream from the blanket heats to 646ºC, which is an attractive outlet temperature for power conversion. We estimate the power conversions efficiency to be 49%. A one-dimensional model that accounted for both the inboard (IB) and outboard (OB) was used in the neutronics analysis that gave the tritium breeding ratio of about 1.22, which seems to be adequate in meeting tritium self-sufficiency goal.

2.3 ITER Test Blanket Modules for Tritium Supply and High Temperature

Around 2003, the US made the decision to re-enter the ITER project. The APEX study was concluded at this time and the focus of the research program again turned to the definition and development of the Test Blanket Modules for US favored concepts. A new study was initiated to perform a technical assessment of the available data and analyses to date and the following choice of preferred US concepts and strategy was developed:

- A helium-cooled solid breeder concept with ferritic steel structure and beryllium neutron multiplier, but without an independent TBM
- A dual-coolant Pb-Li liquid breeder blanket concept with self-cooled LiPb breeding zone and flow channel inserts (FCIs) as MHD and thermal insulator

For both concepts a strategy is being developed emphasizing international collaboration on all aspects of the TBM R&D, mockup testing and TBM fabrication, qualification and operation. Among the specific objectives of ITER testing are:

- validation of structural integrity theoretical predictions under combined and relevant thermal, mechanical and electromagnetic loads;
- evaluation of uncertainties of tritium breeding predictions;
- validation of tritium recovery process efficiency and T-inventories in blanket materials;
- validation of thermal and fluid flow predictions for strongly heterogeneous breeding blanket concepts with surface and volumetric heat sources;
- information on first effects of radiation damage on component operation and first information on integrated

component reliability;
- information leading to the demonstration of the integral performance of the blankets systems.

TBMs will be inserted in ITER from before Day 1 of operation. Very important information will be obtained from TBMs before and during the H-H phase; for example:

- demonstration of the structural integrity of the TBM structures and attachments during disruption and Vertical Displacement Events (VDE);
- assessment of the impact of Ferritic/Martensitic steel, used as a structure for most TBMs, on magnetic fields deformation in static conditions;
- testing of fluid flow, particularly MHD, in the complex 3-component magnetic field environment;
- establishment of TBM first wall requirements, *e.g.,* the need for beryllium coating;
- screening of flaws in TBMs so that they can be fixed prior to D-T operation.

It should be noted that ITER-FEAT operating parameters such as wall load, neutron wall load, plasma burn and dwell times, and fluence were reduced significantly in an effort to reduce overall costs during the period of the Extended EDA while the US was not involved. This reduction in operating parameters led to testing limitations in terms of providing all the required conditions to develop blankets for DEMO. However, ITER is currently the only planned fusion facility in the world fusion program over the next two decades that can provide an integrated fusion environment for blanket and material testing. Therefore, maximum utilization of ITER for blanket and material testing is essential for the advancement of energy related fusion technology that in turn provides essential feedback to possible plasma physics operating regimes and boundary conditions.

2.3.1 Choice of the US Liquid Breeder Blanket Option

In the US study of options, liquid breeder blanket options were evaluated taking into account R&D results from the world program over the past decade. These options include:

- self-cooled lithium with vanadium structure (Li/V);
- helium-cooled lead-lithium (HCLL) with ferritic steel structure;
- dual coolant lead-lithium (DCLL) with He-cooled ferritic steel structure;
- self-cooled and dual coolant molten salts with ferritic steel structure.

Although the Li/V concept was the US favored concept for two decades, it was not selected for the US TBM because of seriously negative R&D results. In particular, the lack of progress on developing practical MHD insulator coatings with acceptable crack tolerance makes the Li/V not a suitable candidate for ITER TBM testing. There are also concerns about V alloy development cost and time schedule. The helium-cooled lead-lithium alloy 83Pb-17Li (referred to in this paper as PbLi) option is being developed by the EU. It has some attractive features as a near term option but its thermal efficiency is limited and there are issues of tritium permeation and corrosion.

Many earlier studies concluded that reduced-activation ferritic/martensitic steel like EUROFER97 or F82H (referred to in this paper as FS) is the only attractive and practical structural material that is available in the ITER testing time frame. The US has decided to focus on testing Dual-Coolant liquid breeder blanket concepts (with ultimate potential for self-cooling) in order to obtain relatively high thermal efficiency while using FS as the structural material. In the dual coolant concept, the helium cooled ferritic structure is always kept below 550°C, which is the FS operating limit based on yield strength considerations. The liquid breeder is "self cooled" and has an exit temperature substantially higher than that of the structural material. Two liquid breeders were evaluated: PbLi, and the low melting point molten salts $LiBeF_3$ and FLiNaBe. In the end, the DCLL concept was selected as the primary candidate for testing in ITER, with dual-coolant molten salt as the backup option.

The DCLL concept proposes the use of a flow channel insert (FCI) made of SiC_f/SiC composite in the breeder region flow channels in order to:

- thermally insulate the self-cooled breeder region from the helium cooled FS walls;
- electrically insulate the PbLi flow from current closure paths in the FS walls;
- provide a nearly stagnant PbLi layer near the FS wall that has increased corrosion temperature limits.

The FCI geometry is shown in Fig. 5, where a typical breeder unit cell is shown. The FCI has roughly a "C" shape, with

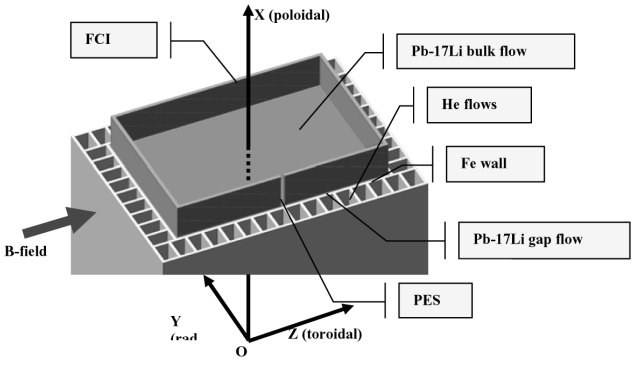

Fig. 5. Typical Poloidal Blanket Channel with FCI and Helium Cooling Channels.

a gap provided to allow pressure equalization from the interior region to the exterior of the FCI near the wall. Since electric circuits must be continuous, a single gap is still allowed from the perspective of electrical insulation. The flow is oriented poloidally, generally flowing one direction near the first wall, turning 180°, and returning in the rear of the blanket.

The FCI improves performance of the DCLL blanket over separately cooled PbLi blankets by allowing higher outlet temperature from the self-cooled LM breeder zone, increasing overall energy conversion efficiency. This high temperature is possible because all structures are separately cooled by helium, eliminating any requirement for the PbLi region to be colder than the structure to promote heat transfer from the wall to the LM. With the thermal insulation provided by the FCI, the bulk PbLi temperature (in the interior of the FCI shown in Fig. 5) can in fact be significantly higher than the wall temperature, provided that the FS/PbLi interface temperature is kept below corrosion temperature limits for FS. Current designs have the bulk PbLi exit temperature at ~700°C, with peak PbLi temperatures near 800°C in the front channels near the first wall.

The FCI also serves to significantly reduce the degree of MHD pressure drop when compared to that of a purely self-cooled design. The fact that a high PbLi velocity is not needed for first wall or other structure cooling, combined with the high PbLi temperature change allowed due to the thermal insulation provided by the insert, results in a very low mass flow rate required to remove the nuclear heating in the self-cooled PbLi channels. This low velocity reduces the MHD pressure drop by roughly an order of magnitude when compared to bare-wall self-cooled designs (the degree of reduction depends somewhat on geometry and loading assumptions, but this is a rather conservative estimate). In addition, the electrical insulation provided by the FCI can reduce the pressure drop by another factor of 3 to 100 or more, depending on the electrical conductivity and thickness of the SiC FCI and steel wall. Together, these two effects are sufficient to keep wall stress below material limits of the FS, even in long, high field, inboard blanket channels where very high pressure stresses can be generated for LM blankets.

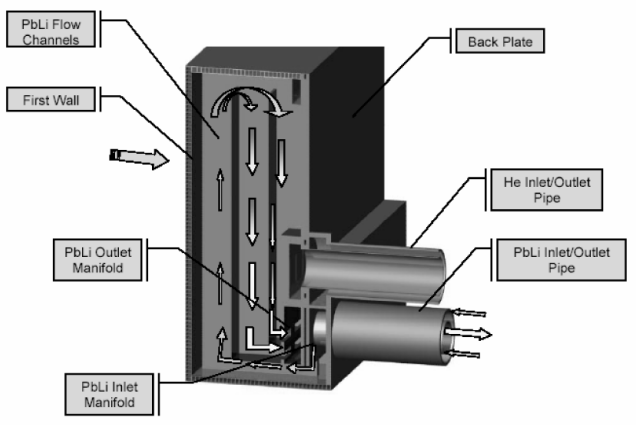

Fig. 6. Typical DCLL Blanket Configuration

The main design features of a DCLL blanket are illustrated in Fig. 6 (for details of the ITER DCLL TBM see [26]). For example, in the DEMO design, the breeder is heated from 460°C to 650-700°C by absorbing neutron volumetric heat while doing two poloidal passes through the module. In the DEMO design, the PbLi circulates slowly (~10 cm/s) making an upward poloidal pass of about 2 m and then flowing downward through two poloidal return channels. With the use of multiple-reheat Brayton closed cycle gas turbine power conversion system [27], the temperature difference of 200-250°C will result in a gross power conversion efficiency of 40% or higher. Another important blanket characteristics is the overall tritium breeding ratio estimated to be 1.15 using Li^6 enrichment [26].

3. SELECTED EXPERIMENTS AND MODELING RESEARCH PROGRESS

A significant amount of research, development and design was carried out in the US technology programs described in the preceding section. Here we give some detailed examples of some of these research areas with particular focus on the thermofluid and thermomechanical issues associated with both innovative and more conventional blanket systems.

3.1 Free Surface Flow Research for Liquid Walls and Divertors

The APEX study had focused a significant amount of attention on the possibility of utilizing flowing liquid layers as a virtual first wall in magnetic fusion reactors. Such a concept requires that the liquid layer absorbs energy from the plasma in the form of radiation and energetic charged and neutral particles. The flow behavior and heat transfer of the liquid wall flows are very different depending on whether the working liquid is a low conductivity molten salt or a high conductivity liquid metal. Significant research on both types of fluids was carried out under APEX, and at some smaller level liquid metal free surface flow modeling and experiments are continuing today to evaluate the feasibility of placing a liquid metal free surface divertor experiment into the National Spherical Torus Experiment (NSTX) [28].

3.1.1 Free Surface Modeling and Experiments for Low Conductivity Fluids

As an example liquid wall design using a molten salt

as the working liquid in the CLiFF thin wall configuration we refer to the concept detailed in Ref. [21]. The free surface in the CLiFF flows is exposed to a high surface heat flux (~2 MW/m^2) from the plasma and is affected by a strong reactor magnetic field (~10 T). A key thermofluid issue for molten salt flows under CLiFF parameters is the minimization of the surface temperature, and thus the amount of evaporated material that could potentially enter and poison the plasma. This surface temperature is critically related to the heat transfer at the free interface facing the plasma heat flux.

Molten salt flow and heat transfer differs from liquid metals in profound ways. Molten salts typically have low thermal conductivity and so heat transfer through the flow is highly dependent on the level of turbulence. Near the free surface this turbulent transport process is known as "surface renewal" – where liquid from the flow interior is delivered to the free surface by turbulent eddies [29]. The turbulence motion itself will be affected both by the proximity of the interface and the strength of the magnetic field. To address issues associated with the turbulent free surface flows of molten salts a number of studies were performed – both theoretical and experimental. The primary goal of the research was to develop a predictive capability for calculating velocity and temperature fields in low conductivity fluid flows under conditions relevant to fusion systems. The theoretical studies included the implementation of MHD effects and those related to the free surface phenomena into the so-called "K-ε" model of turbulence. The experimental studies were aimed at understanding and classifying free surface phenomena related to the interaction of the bulk turbulence with the free surface and associated wavy phenomena. Through this, it was possible to evaluate K-ε model coefficients, which were needed to close the turbulence model. The practical importance of the model developed is that it has been brought to a complete form, so that using it in heat transfer calculations does not require any additional information. The corresponding studies are described below with some typical calculations of heat transfer. A detailed description of the research and applications to liquid wall flows can be found in Refs. [30-32]

The starting point in the development of this turbulence model is the standard set of the flow equations for incompressible liquids, known as the Navier-Stokes equations, along with the energy equation and equations for electromagnetic quantities known as the Maxwell equations. The electromagnetic equations have been added since suppressing turbulence by a magnetic field through the dissipation of mechanical energy into the Joule heat is one of the key physical mechanisms. The turbulent flows can be analyzed by using these equations through the so-called Reynolds decomposition, *i.e.* dividing the flow and other parameters into mean and fluctuating parts. After decomposing, the equations are averaged in the long time or ensemble average sense. The equations obtained in this way include new terms, which consist of unknown correlations. In order to get a closed set of equations, these new unknowns need to be modeled. In the present studies these relations were developed based on the results of Direct Numerical Simulations (DNS) [33] along with the well-documented experimental data for MHD channel flows. Unlike the classic K-ε model, the present one incorporates the most important MHD phenomena and can be applied to low conductivity fluid flows for different orientations of the applied magnetic field.

Experiments with inclined open surface water flows heated from the free surface side [32] were performed to help determine the range of applicability of the K-ε model as a tool for calculating hydrodynamic quantities (such as the mean flow thickness) and heat transfer. Another goal of the experimental effort was to evaluate the effect of surface disturbances (which are quite likely to appear under CLiFF conditions) on heat transfer. The experiments were conducted using a water loop since the physical properties of the molten salts of interest do not substantially differ from those of water. The test section is a 4-m long, 40-cm wide inclined flume. The fluid is injected continuously into the test section by two centrifugal pumps through an adjustable nozzle. An infrared (IR) heater is used to heat the liquid from the side of the free surface. The measurements include IR images from the infrared camera, as well as the flow thickness versus time measured by the ultrasound transducer. The relevant parameters, the Reynolds number (*Re*), the Froude number (*Fr*), and the Weber number (*We*) were chosen to match those in the FLiNaBe liquid wall design.

An example of experimental data is shown in Fig. 7. The experimental data were treated statistically. By analyzing the statistical characteristics of the flow, such as the mean flow thickness, standard deviation, probability density function, and power spectral density, a key role of the Froude number has been revealed. As *Fr* grows, the wave amplitude grows, and the frequence spectrum shifts towards shorter waves and more intensive mixing at the surface occurs. The surface disturbances observed in the experiments are mostly related to the interaction of bulk eddies with the free surface and lead to heat transfer improvement by up to two times [34]. Another important conclusion from the experiment is that under the CLiFF conditions the free surface will be agitated but not broken into droplets. This regime is known as transitional from "weak" (no surface disturbances) to "strong" turbulence (the surface is broken). The experimental data for the flow thickness and those for heat transfer were also used in the comparisons with the theoretical predictions. In the range of flow parameters relevant to the CLiFF design, the agreement was pretty good.

The present K-ε model was used to calculate the hydrodynamics of the flow down the structural wall using FLiNaBe as a working fluid. Different flow regimes were calculated for thick and thin flows (Fig. 8) in the presence of a strong

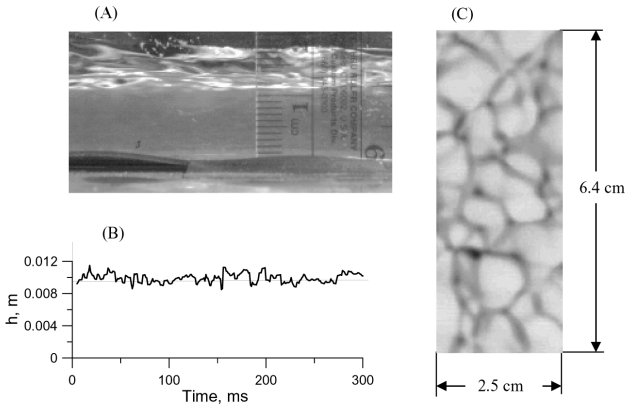

Fig. 7. Water-Air Interface in the Regime from "weak" to "strong" Turbulence: Flow Inclination is 3.5°; Velocity is 1.43 m/s; Mean Flow Thickness is 0.0093 m. (A) The Flow as Viewed from the Side Through the Transparent Side Wall. Two Distinct Layers can Be Seen. The Upper Layer is the Intermittence Region Occupied by Water and Air, While the Lower Region is Filled with Water Only. (B) Time Variations of the Flow Depth Measured with the Ultrasound Transducer at a Point Location, 3.5 m Downstream of the Nozzle at the Middle of the Flume. (C) A Picture Taken from Above the Free Surface Shows Cell-Type Structures at the Surface, which Appear Mostly as a Result of Turbulence-Interface I nteractions

10 T magnetic field. The thick flows experience significant gravitational contraction. The MHD effects on the mean flow were found to be negligible because of a low electrical conductivity of FLiNaBe and also due to the fact that solid walls perpendicular to the toroidal magnetic field are not present. A thin flow first wall flow with properly chosen initial velocity and height demonstrates very uniform depth/velocity distributions over almost the entire flow length. One of the cases calculated, with the inlet velocity, U_0, of 10 m/s and the inlet flow thickness, h_0, of 2.3 cm, demonstrates almost no variations. This flow regime has been chosen as a working regime in the FLiNaBe design.

The model was also used to calculate the downstream changes of the surface temperature in the FLiNaBe liquid wall flows. The surface heat flux distribution adopted in the present calculations underlines the basic features of the real heat flux distribution in the outboard region by using a step-type function. The heat flux of 1.4 MW/m^2 is applied over the First Wall area, jumps to 12 MW/m^2 over a 2-cm section within the divertor region, and then drops down to 1.4 MW/m^2 again. The flow scheme presently considered assumes a continuous flow over the whole area when the liquid flowing over the first wall enters the divertor area without additional mixing. The results of heat transfer calculations are shown in Fig. 9 in the form of the surface temperature rise (T_s-T_0) versus the distance along the reactor wall, where T_0 is the surface temperature and T_s is the inlet temperature. The figure also demonstrates the effect of surface waves (disturbances).

3.1.2 Free Surface Liquid Metal Experiments

In the MTOR facility at UCLA [19,35], 24 coils form a magnetized toroidal volume which has a circular cross-section with major/minor radii R = 0.78 m and a = 0.39 m. The facility supports testing of liquid metal free surface flow concepts without the technical complications and constraints of plasma. The magnetic system is coupled with a liquid metal flow loop utilizing 15 liters of the GaInSn alloy (Ga-67%, In-20.5%, Sn-12.5%) and with

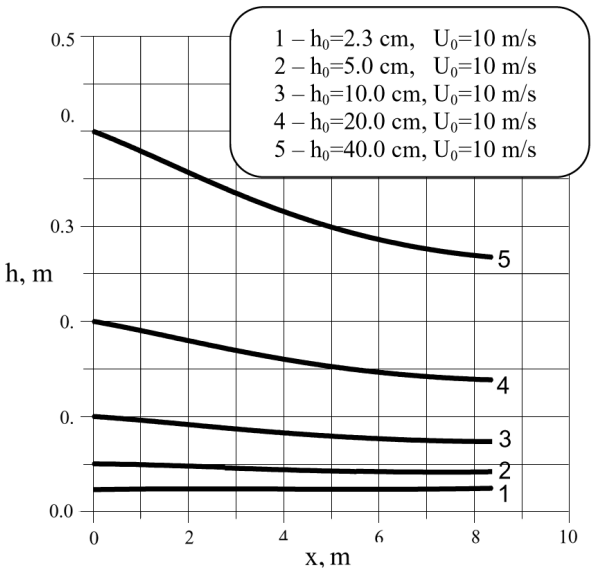

Fig. 8. Downstream Changes of the Flow Thickness for Thick and Thin Flows Calculated with the K-ε Model

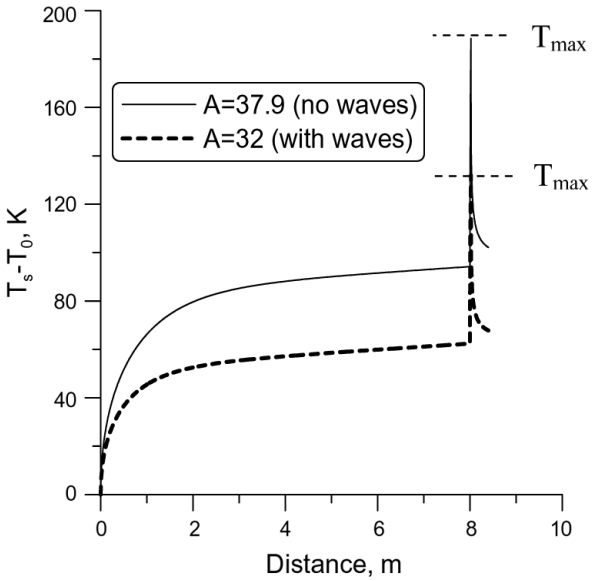

Fig. 9. Surface Temperature Rise Over the First Wall / Divertor Area.

an annular induction-type electromagnetic pump with variable flowrate control. A cover gas / vacuum system allows control of the atmosphere in the loop and attached test articles so that the GaInSn sees an inert environment to reduce oxidation and contamination of the alloy and allow experiments at different background atmosphere pressures. The facility is shown in Fig. 10.

The research effort at UCLA has been actively studying the behavior of free surface liquid metal flows under fusion relevant magnetic fields. There is a particular interest in studying the behavior of liquid lithium streams, flowing at a velocity of 10 m/s inside the divertor region of NSTX (The National Spherical Torus Experiment at Princeton, New Jersey, USA). The MTOR facilities at UCLA can closely replicate the scaled NSTX divertor region magnetic field conditions by using an assortment of electromagnetic coils and permanent magnets. A scaling factor of 2.0 is multiplied to the NSTX magnetic fields to ensure that the dimensionless Hartmann number remains the same while working with the gallium alloy so that the results obtained could be applied to lithium flows inside the NSTX divertor environment. The Reynolds number is matched by flowing the heavier gallium alloy at lower velocities.

Flow issues for film flows are related primarily to the slowing down and thickening of the flow due to MHD forces, and the penchant for multi-component field with gradients to push the flow to one side or the other of the flow channel. To study these various phenomena many experiments have been performed [19]. The current experimental effort underway in MTOR has an experimental test section that consists of a stainless steel channel with a wall thickness of 0.5 mm. The channel is 40 cm long and 20 cm wide. At the inlet, a nozzle introduces the liquid metal into the channel in the form of a thin stream with a thickness of 2 mm. The entire channel is enclosed in a vacuum box and a constant flow of argon is maintained over the channel. The inlet velocity of the liquid metal film at the nozzle is varied over a range from 1 m/s to 3 m/s. The most critical MHD effects are expected from the wall-normal gradient magnetic field. Permanent magnets placed underneath the channel replicate the scaled NSTX surface-normal field component. The liquid metal film flow exhibits some interesting features. The 2 mm thick film emerging from the nozzle tends to have a rapid increase in thickness at a particular downstream location depending on the initial inlet velocity (Fig. 11). This sudden increase in the fluid film thickness is here referred to as the jump. The higher the initial velocity, the farther is the location of the jump from the inlet nozzle. For an inlet velocity of 1 m/s, the jump is located 7 cm downstream from the inlet nozzle, for an inlet velocity of 2 m/s its location is approximately 15 cm downstream. The principal cause of the jump is the Lorentz force acting on the fluid, against the flow direction. At low inlet velocities the jump is straight across the span but it gets progressively bowed in the spanwise direction as the inlet velocity is increased. This is suggestive of the presence of fast jet like structures close to the side walls, where the local fluid velocity is higher than in the central part of the channel. At an inlet velocity around 3 m/s, an increasing cross-sectional force is observed manifesting in the tendency of the fluid to being pushed away from the side walls of the conducting channel. The surface normal magnetic field component progressively increases downstream and causes the liquid

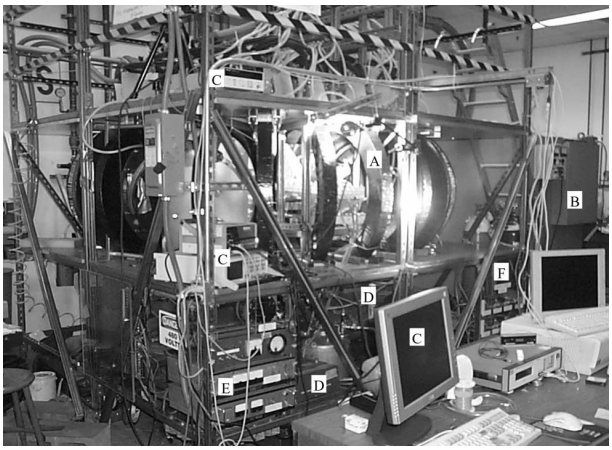

Fig. 10. MTOR Toroidal Magnetic Field/Gallium Alloy Flowloop Test Stand. (A) Magnetic Field Coils, (B) Toroidal Field Coil Power Supply, (C) Computer Controls and Data Acquisition, (D) EM Pump and Pump Controller, (E) Magnetic Propulsion Current Supplies, (F) Cover Gas Controls

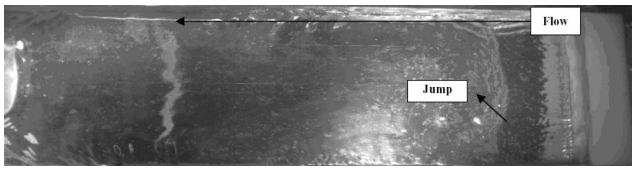

Fig. 11. Film Liquid Metal Flow in a Wall-Normal NSTX-Type Magnetic Field Demonstrates a Rapid Flow Thickness Increase (jump) Caused by the Lorentz Force Acting Along the Flow Direction. Inlet Velocity is 2 m/s. Inlet Flow Thickness is 2 mm, Channel is Electrically Conducting

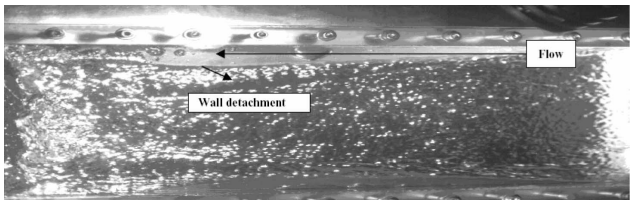

Fig. 12. Flow Detachment from the Side Walls Appears at Higher Flow Velocities. Inlet Velocity is 3 m/s. Inlet Flow Thickness is 2 mm, Channel is Electrically Conducting

metal stream to pinch inward (Fig. 12), trying to change shape to keep the linked magnetic flux constant.

These preliminary data from the MTOR film flow test module shows up to a factor of three times increase in film height as the result of MHD forces. Such a fluid pile-up may not be favored since it would act as a "leading-edge", which would be vulnerable to surface heating and result in excessive vaporization and possibly plasma disruption. Another concern is the pinching effect. This pinching may lead to separation zones or bare spots where the liquid has completely pulled away from the wall. However the flow does not stagnate and is successfully removed from the test chamber. Possibly there is some design that allows the use of fast films without intolerable manifestations, *i.e.*, excessive liquid surface heating.

3.1.3 Free Surface Liquid Metal Modeling

A true resolution of free surface feasibility issues requires advanced modeling of liquid metal MHD flows in a multi-component non-uniform magnetic field with externally applied control currents, 3D geometry, curvatures and penetrations. Ideally, mass, momentum and energy conservation, electromagnetic simulation, and free surface tracking capabilities all should be accounted for in a complete fashion with a minimum of assumptions. In APEX a strategy was adopted to begin development of a 3D simulation tool while concomitantly advancing the simulation capability in reduced dimensions by making use of the approximation of toroidal axisymmetry. In this fashion, we have been continuously increasing our understanding of liquid metal wall flows by modeling more and more complex field and field gradient issues, while working towards the capability needed to simulate complex geometry flows in 3D. In addition, work in 2D and 2.5D could be used for benchmarking the complex 3D simulation tools.

It is fairly easy to see, given the toroidal geometry of a tokamak, that flows along a first-wall could be idealized such that they extend completely unbroken and without variation in the toroidal direction around the axis of revolution of a poloidal cross-section. The assumption that the flow, and the magnetic fields through which the flow must move, have no toroidal variation is termed here *axisymmetry*. The convenience of the axisymmetic assumption is that it decouples the effect of magnetic fields applied in the direction of the axisymmetry (toroidal) from those in the poloidal plane. Several codes and various analytic solutions have been developed that utilize the axisymmetric assumptions and have been applied to the evaluation of the various liquid wall flows and have given great insight into the motion of liquid walls in toroidal and multiple component fields [23, 36-40]. Some of the more interesting conclusions are summarized below.

Analytic solutions of fully developed free surface flow in a toroidal field with constant gradient have shown that an asymmetric M-shaped velocity created, driven purely by the pressure gradient effects associated with the variations in the wall-normal Lorentz force [41]. It is seen that this effect is the result of the same physical effect as the already mentioned magnetic propulsion idea [17] proposed to aid in-situ pumping of free surface flows in fusion reactors. A 2.5D code utilizing height function free surface tracking was developed to model the combined effect caused by the geometrical curvature and the toroidal magnetic field with 1/R toroidal field [39]. Under these conditions, currents induced remain poloidal and the drag they induce slows down the flow. This drag was shown to be not overly significant for thin fast film flows like those being considered for thin flowing first walls. Calculations have been performed for a typical outboard liquid first-wall case in a reactor where the flow will experience an average toroidal field gradient in the range of 0.25 to 1 T/m depending on the first-wall geometry assumed [23]. For a circular arc outboard flow geometry the lithium flow depth is affected only slightly by the field gradient drag effect. However, the drag quickly becomes very large when the desired flow thickness is increased.

The MHD effects become even more unusual as one adds additional field components and observes the interaction of various components of the field and induced currents [23, 39]. For example, when a small wall-normal component of the magnetic field additionally to the toroidal field with 1/R variation is considered, the result is a secondary toroidal flow. In the case under consideration, the secondary flow exists in the form of a swirl flow and is caused by the toroidal Lorentz force, which arises from the interaction between the poloidal currents and the wall-normal magnetic field. Figure 13 illustrates the swirl flow effect. Although the wall-normal magnetic field is very small comparatively to the toroidal field, the swirl flow is pronounced and even comparable with the main flow. Even more interesting is the fact that the toroidal Lorentz forces are oppositely directed near the back-wall and free surface. Correspondingly, the liquid in the layer rotates in two opposite directions with strong shear over the thin layer.

The so-called magnetic propulsion current discussed earlier can be added to improve significantly the flow behavior. Calculations [40-41] and recent experiments [35] have shown this current to be very effective in pushing the liquid against the back wall, aiding in liquid propulsion, and suppressing surface instabilities–potentially overcoming several of the problems discussed above. The most serious problem encountered with the magnetic propulsion idea is the effect of other field components on the flow dynamics. The use of streamwise magnetic propulsion currents in a case with a wall-normal field component will preferentially push the liquid in the toroidal direction. For an axisymmetric flow, these types of toroidal motions are acceptable. But if one considers toroidal breaks of any kind, liquid splashing and non-uniformity can result. Also in a design that realizes the magnetic propulsion idea, there are concerns related to the injection and extraction of the liquid metal in and from the reactor chamber.

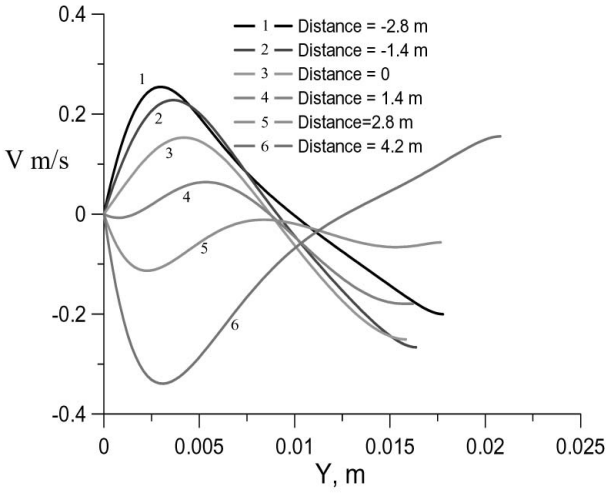

Fig. 13. Toroidal Velocity Profiles Over Liquid Depth for Liquid Sn Flow in Toroidal Field Gradient and Constant Radial Field (0.05 T)

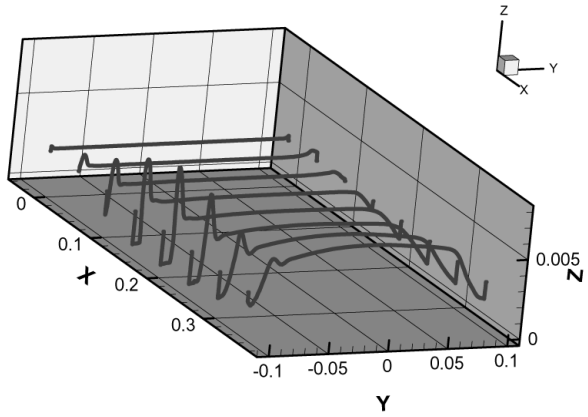

Fig. 14. HIMAG Calculations of the Liquid Metal Film Flow in a Wall-Normal NSTX-Type Magnetic Field. The Flow Detachment Effect is Seen as the Flow Proceeds Downstream

It was recognized by the conclusion of the first phase in APEX that a numerical tool that can handle complex 3D geometry free surface MHD flows would be indispensable to the understanding of liquid wall flows. It was also recognized that it would take considerable effort to develop such a capability, and even if successful, the code might be very limited in the range of Hartmann number if steps were not taken in the beginning to overcome as much as possible inherent limitations in formulation or numerical methodology. So the design of a new numerical tool specifically formulated to overcome the limitation of existing tools was initiated. In this way, the HIMAG (HyPerComp Incompressible MHD solver for Arbitrary Geometries) code [42] was initiated with the following principles:

1. Unstructured grid formulation to allow any geometry of fluid flow, nozzles, obstructions, *etc*. to be accommodated, and to allow high resolution of thin Hartmann type boundary layers at high Hartmann number with a minimum of cells.
2. Parallel solver implementation to allow large problem sizes and "stiff" matrices to be solved in an acceptable amount of wall clock time.
3. Flexible implicit framework for using various free surface tracking (level-set, VOF, *etc*.) and electric current (potential formulation, induced-B formulation, *etc*.) modules and for reducing time-step restrictions

In its present form, the following capabilities are available in HIMAG:

- Three dimensional incompressible flow solver,
- Free surface capture using level set technique,
- Arbitrary mesh structure (unstructured/hybrid),
- Parallel code environment using MPI,
- Computation of electromagnetic fields using the electric potential formulation,
- Multiple strategies to solve for Poisson equation matrices
- Multiple strategies to account for mesh skewness (non-orthogonality),
- Modular addition of source terms,
- Graphical user interfaces.

Many benchmark cases have been performed to help improve and debug the code [36]. While the HIMAG code has just recently neared the production stage, there have been a lot of efforts to simulate different experimental tests currently underway. The numerical modeling is expected to help in a better interpretation of the experimental findings as well as help to gain new insights and probe in directions missed out by the experiments. HIMAG was used to simulate the various experiments in MTOR with gallium alloy flow, using the geometry and the magnetic field distribution of the experimental set up described above. The case with an inlet flow velocity of 3 m/s was selected for comparing the experimental and numerical results. Only the first 20 cm of the channel flow length was simulated. The solid channel was meshed with cells having the electric conductivity of stainless steel. The simulation predicts that the MHD body forces cause the liquid metal film to thicken by an order of 1 mm at 16 cm downstream into the flow. This matches well with the experimental value of an increase by 1.3 mm at the same location.

In another simulation, the behavior of a lithium stream with an inlet velocity of 10 m/s and inlet film thickness of 2 mm, flowing under the three component NSTX divertor region magnetic field, was studied. The lithium stream was supported by a 40 cm $\times$ 20 cm stainless steel substrate with a wall thickness of 0.5 mm, which formed a part of the computational domain to simulate the induced current

closure paths through the conducting walls. The flow was set to climb a slope of 21°, as in the actual design proposed for the NSTX module. Figure 14 shows the variation of the film thickness in different cross-sections along the flow path. It can be seen that the spanwise variation of the film thickness is highly asymmetric about the centerline. It is seen that the flowing film has a tendency to 'pinch in' and it detaches from one of the side walls as the flow progresses downstream, similar to the experimental observations.

3.2 Solid Breeder Thermomechanics

The thermo-mechanical performance of lithium-based ceramic materials is a critical issue for assessing the reliability of solid breeder blanket concepts over the lifetime of the component. The investigation of the effect of the thermal cycling typical of a fusion energy power plant on the blanket components is complicated by the coupling of the thermal and structural behavior intrinsically related to the use of pebble beds as breeding material. The pebble bed as a whole can be described as an intermediate phase between solid and liquid, with properties depending on the fraction of voids present in the bed volume. The void fraction initially depends on the porosity and the initial packing of the pebbles, but can vary locally through the component lifetime due to the cycling variation of the applied stresses and to irradiation. For example, the formation of a void between the pebble bed and the structure due to creep relaxation would lead to a local deterioration of the interface heat transfer and the creation of a hot spot. The effect of thermal cycling is further aggravated by the degradation of materials mechanical properties due to neutron irradiation, and final assessment of blanket component reliability will only come from an integrated experiment such as ITER.

Various approaches have been pursued devoted to the development of predictive capabilities of time-dependent thermomechanics interaction and corresponding stress and strain deformation histories of ceramic breeder pebble beds. This includes both finite element and micromechanical models as well as empirical constitutive equations. Although significant progress has been made worldwide, a complete knowledge of the phenomena is still not yet fully available [43-45]. This is due not only to the lack of a detailed description of material properties, but also, the significant amount of parameters involved in the phenomena ranging from materials, microstructures and sizes of particles, non-uniformities and asymmetries in physical phenomena, and loading histories that are experienced by particles, *etc*. There is no doubt that a predictive capability based on finite element approaches is essential due to the ease with which they can be applied to a large scale design analysis. However, in order to simulate the process, constitutive models, which show how pebble bed properties change with pressures, temperatures and loadings are needed. The discrete element method is based on the concept that each individual particle is considered to be separate and is connected only through the contact by appropriate physically-based interaction laws. It provides insightful information at the inter-particle contact, including the likelihood of particle breakage. Example calculations based on different modeling approaches are presented in the following sections.

3.2.1 Deformation Mechanisms and Experimental Observations

Although the maximum macro-scale thermal stress exerted on the particle bed due to differential thermal expansion can be relatively moderate, such as 2.0 MPa, this small stress magnitude can significantly be magnified to hundreds of MPa initially at particle/particle contacts as a result of small contact areas, and decreases to tens MPa once the deformation starts [46]. As pressure is applied, the effect of high temperatures is to promote inter-particle mass transport, which results in deformation starting with the contact. In general, deformation for ceramics can be evaluated by the sum of linear and power-law creep terms [47]:

$$\dot{\varepsilon} = A_1 \exp(-Q_1 / RT)\sigma + A_2 \exp(-Q_2 / RT)\sigma^n \qquad (1)$$

where A_i*s* and Q_i*s* are material properties and are functions of grain size, particle density, fabrication techniques, *etc*., T is temperature in K, σ is the von Mises stress in MPa, n is the stress exponent and $\dot{\varepsilon}$ is the creep rate in s^{-1}. A stress exponent of around 6.5 was found [47]. In a previous analysis, creep rate as a function of time derived experimentally for a Li_4SiO_4 particle bed and extrapolated to individual particles [48], was used in the discrete element code to benchmark against experimental observations. As shown in [46], the calculation simulated well the time dependent aspect of deformation characteristics but predicted a smaller amount of deformation as compared to the experimental results. The quest to obtain correct material creep properties in order that the DEM code can be effective has warranted experimental study of time-dependent creep deformation on two particles. An experimental study of this phenomena is currently under way at UCLA.

The growth of the contact radius causes bed compaction, which reduces the overall bed thermal strain and associated stress. Imposing volume conservation and geometrical constraints, the compaction along the center of the axis between two neighboring spheres (d) after creep formation can be evaluated as [49]:

$$\delta = (a+b) - \frac{2}{3}\left[\frac{a^3+b^3}{r_{c,0}^{\ 2}} + \left(1 - \frac{a^2}{r_{c,0}^{\ 2}} - \frac{b^2}{r_{c,0}^{\ 2}}\right)\left(\sqrt{a^2 - r_{c,0}^{\ 2}} + \sqrt{b^2 - r_{c,0}^{\ 2}}\right)\right] \qquad (2)$$

where a, b are the radii of the two touching spheres and $r_{c,o}$ is the contact radius at the previous time step.

3.2.2 Discrete Element Method Calculations

An advantage of discrete element simulation is its ability to trace the evolution of contact characteristics and forces as deformation proceeds. As shown in Fig. 15 (A), the force distribution at the contact is illustrated where the line thicknesses reflect the force magnitudes. These forces – emerging from the propagation of stress at the particle-wall contact, which is caused by initial strain deformation due to temperature rise, difference in thermal expansions and bed relocation – begin to relax as the creep becomes significant. Figure 15 (B) illustrates the force distributions after thermal creep is initiated. In comparison a force reduction due to creep relaxation is clearly seen.

3.2.3 Finite Element Simulations

The finite element method considered in this paper is similar to the method developed at NRG [43], where stress and strain magnitudes for a typical ceramic breeder unit are calculated using the commercial code MARC [50] incorporated with experimentally derived consitutive creep deformation models [51-52]. In a macroscale finite element analysis, the pebble bed is treated as a continuous material with the effective thermo-physical and mechanical properties. It relies on accurate micromechanical models and empirically derived and validated constitutive equations for modulus and stress-strain relationship. The objective of the analysis is to characterize the general behavior of the pebble bed as a function of time, and specifically to look at the effect of creep compaction on stress relaxation and the possible formation of gaps between the pebbles and the structure, which could lead to the formation of hot spots. The effective elastic modulus and creep compaction of ceramic breeder (E_C and ε_C) and beryllium (E_B and ε_B) pebble beds are related to stress and temperature levels by the expression [48, 51-52]:

$$E_C = 314x\sigma^{0.75} \text{ and } E_B = 1772x\sigma^{0.83} MPa \qquad (3)$$

and

$$\varepsilon_C = 1.6x11.41x(\sigma)^{0.4} t^{0.2} e^{\frac{-9741}{T}} \text{ and}$$

$$\varepsilon_B = 6.40\varepsilon_C \qquad (4)$$

where σ is the axial stress in MPa, T temperature in °C, and t time in seconds.

An example calculation has been performed for a breeder/beryllium unit representing a sub-unit found in the edge-on design blanket configuration in addition, with an attempt to minimize the use of beryllium by increasing the breeder width as it moves toward the back of the blanket region (Fig. 16). As shown, the calculation domain represents half of the unit cell breeder unit using symmetric boundary condition at the center line of the second breeder pebble region. The unit cell is designed to address the issue associated with the pebble bed thermomechanical integrity [53]. The calculated stress profiles at the *x-y* plane of this sub-unit resulting in a combined effect of temperature gradient, differential thermal expansion and structural constraint is shown in Fig. 17. Without taking into account thermal creep effect, the calculated von Mises stress profile of this sub-unit, resulting from a combined effect of

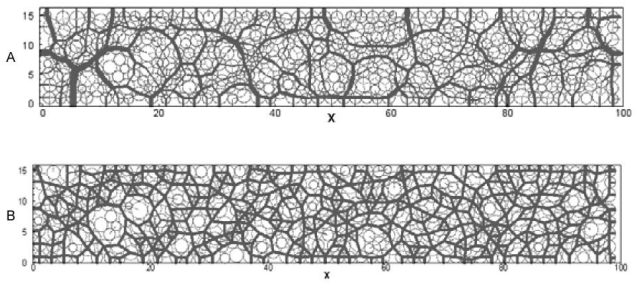

Fig. 15. Force Distributions at Breeder Particle Contacts Based on a Discrete Element Micromechanical Modeling Technique Similar to Molecular Dynamics. The Width of the Contact Lines Reflects the Contact Force Magnitude. Stress Accumulated at the Pebble Contacts (A) is Able to Relax After Onset of Creep Deformation (B)

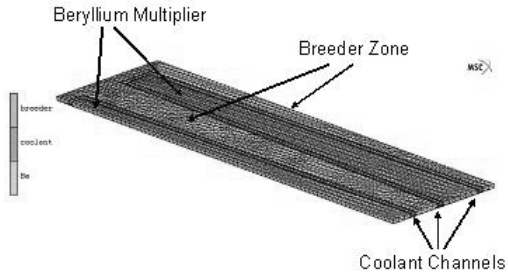

Fig. 16. Calculation Model for a Breeding Blanket Unit Cell Including Breeder and Beryllium Multiplier Zones as well as the Coolant Channel Structures

Fig. 17. Calculated Von Mises Stress Profile in the Breeding Unit (emphasizing stress distribution inside the breeder zone.)

temperature gradient differential thermal expansion and structural constraint, shows a maximum stress level of greater than 10 MPa located inside the beryllium pebble bed near the coolant plate. Whether or not this high stress is accurately predicted is the subject of the current research effort. The maximum stress inside the breeder pebble bed of 1.0 MPa is found ~6.5 cm away from the first wall. The stress profiles at the centerline of the breeder zone as a function of distance at different burn times is shown in Fig. 18 for analyses with creep and without creep. The peak stress level drops to 0.5 MPa at the end of the ITER burn cycle when the thermal creep is coupled into the analysis.

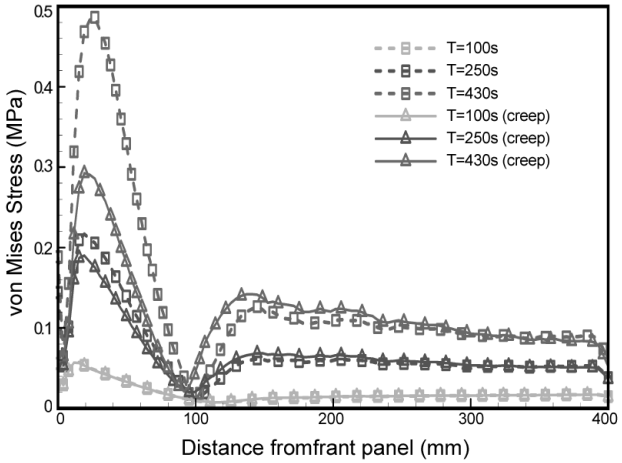

Fig. 18. Calculated Stress Histories Along the Centerline of the Breeder Pebble Bed with and Without Thermal Creep Effect

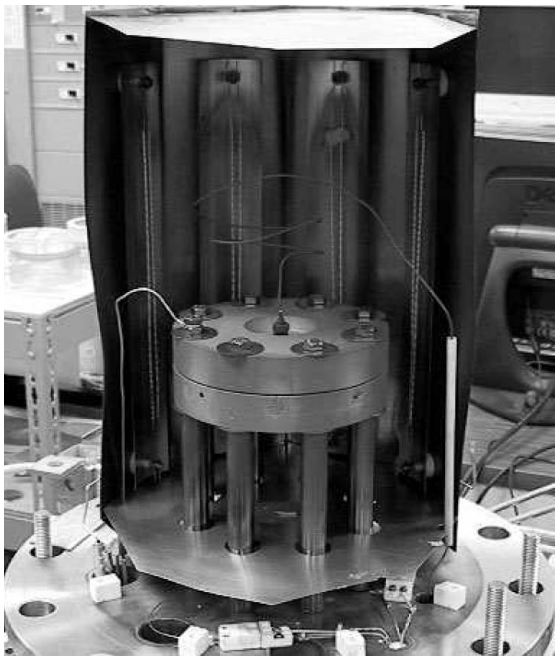

Fig. 19. Test Article Inside High Temperature Furnace

3.2.4 Experimental Study of Ceramic Pebble Bed Systems

The focus of the experimental work initiated at UCLA is the investigation of the combined thermal and structural response of blanket candidate materials exposed to thermal cycles that are representative of fusion energy power plant conditions. In particular, the study is aimed at characterizing the thermo-mechanic performance of various structural, cladding and breeding materials for fusion energy blankets. Specifically, the results obtained with a test article that integrates lithium meta-titanate oxide (Li_2TiO_3) as breeder, silicon carbide as cladding and a low thermal expansion alloy (Kovar) as the structure, as shown in Fig. 19, is described here [54]. The choice is motivated in part by the ongoing research effort under the JUPITER II collaborative program that is aimed at the development of high temperature gas-cooled blanket systems with coolant output temperature as high as 900°C [46].

As the temperature increases, the pebbles act on the SiC disc because of the higher thermal expansion. As a result, the disc bends, and the capacitive sensor embedded in the upper flange reads the maximum displacement at the plate center. The analysis of the experimental results is complicated by the fact that the sensor is not an absolute reference, since it is mounted on a structure also subject to deformation. The effect of the expansion of the sensor (which has a stainless steel enclosure) and the alloy structure in which is embedded was evaluated by testing the assembly without a compressive force, and the resulting deformation was measured to be less than 40 microns, and constant after 600°C. This effect is responsible for the initial increase of the measured gap observed in the data. Figure 20 shows a representative set of data from the first (# 0) and second (# 1) thermal cycles of a thermo-mechanics experiment with the described test article. At low temperatures the expansion of the pebbles is countered by that of the flange on which the measuring sensor is embedded. During the first cycle at temperatures above 700°C, the gap is gradually reduced by about 580 microns due to a combined effect of thermal expansion and pebble rearrangement in the bed. After about 3 hours from the start of the heating cycle and 30 minutes at a constant temperature of 800°C, the effect of the stress relaxation due to the thermally-induced creep in the ceramic material becomes visible, and the gap increases logarithmically at constant temperature to an asymptotic value 120 microns smaller than the initial value, which is completely recovered after cooling indicating that the disc is again straight. The bed height after the second cycle was measured to be about 200 microns smaller than its initial value, accounting for

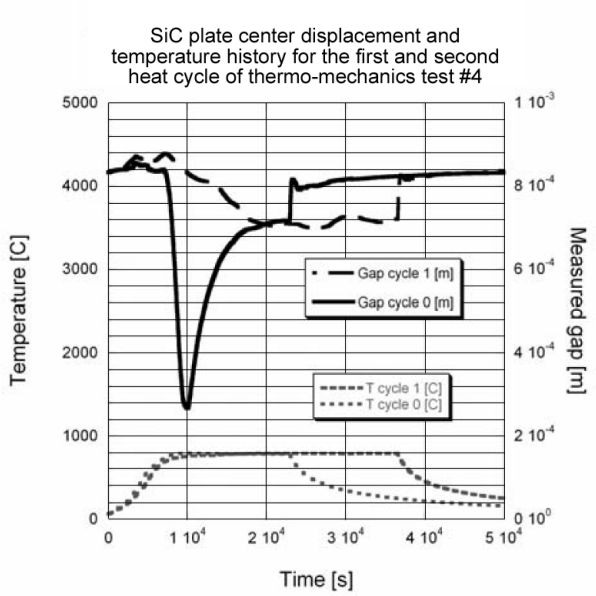

Fig. 20. Displacement Data from Two Heat Cycles of Test #4

an effective residual volumetric deformation of about 1.3%. During the second cycle it is seen that the pebbles have already been compacted and the gap reaches the same asymptotic value without the initial swelling. Further consecutive thermal cycles of the same materials have been performed after re-arranging the pebble bed to recover the initial compressive load. The results are similar to the second cycle showed in Fig. 20, with the exception that the asymptotic value is lower due to the higher initial stress, ranging between 250 microns and 150 microns lower than the initial value.

The experimental results indicate that high thermal stresses and deformations are present during the initial thermal cycle of the assembled test article, but are successively accommodated due to a combination of pebble re-arrangement within the bed and creep-induced deformation. This suggests that a few thermal cycles under controlled atmosphere and a compressive load before final assembling of blanket sections would allow for a beneficial reduction of the swelling and related thermal stresses during start-up.

3.3 Closed Channel Liquid Thermofluid MHD

In support of the ITER Test Blanket Module (TBM) program, the US team has been focusing on the Dual Coolant PbLi (DCLL) liquid breeder blanket option. The DCLL concept has been explored for several years in the US [55-56] and in Europe [57]. At present, the concept is applied to the US reference (DEMO) blanket design and to the ITER TBM. A set of the reference blanket parameters in the steady-state operation regime includes a maximum neutron wall loading of 3 MW/m^2 and a maximum surface heat flux of 0.5 MW/m^2. In the ITER TBM, during the D-T phase, typical operating conditions include a surface heat flux of 0.27 MW/m^2, a neutron wall load of 0.78 MW/m^2, and a pulse length of 400 s with a duty cycle of 22%. Because of possible plasma perturbations, it is however required to design the TBM for a surface heat flux of 0.5 MW/m^2. In the H-H phase, the typical surface heat flux is about 0.11 MW/m^2, and the TBM needs to be designed for a value of 0.3 MW/m^2.

The FCI is one of the most important elements of the DCLL blanket design. It is located in the blanket channels floating in the liquid metal. There is a thin (about 2 mm) gap between the ferritic wall and the FCI. The gap is also filled with PbLi, which is driven by the same pressure head as the liquid metal in the duct. The functions of the gap are to equalize the pressure between the two FCI sides, thus avoiding major primarily stresses on the insert, and to accommodate any thermal expansion and radiation-induced swelling of the insert. The pressure equalization can be provided via the liquid flows through special openings in the FCI, or even without them via electromagnetic coupling between the flow in the duct and that in the gap. (The latter solution still needs to be confirmed either by numerical calculations or/and experimentally). The pressure equalization openings can be made in the form of a long pressure equalization slot (PES) or as a number of small pressure equalization holes located in one of the FCI side (PEH). Although the FCI does not carry significant primary stress, it still carries secondary thermal stresses and its own weight floating in the liquid metal. As mentioned, the effectiveness of the FCI depends on the extent to which the insert can reduce the MHD pressure drop and thermal losses in the helium cooling channels. To address these issues, detailed MHD/thermal analysis was performed in [58-59] for a 2 m front poloidal channel and is also reviewed below.

The mathematical model used assumes fully developed flow conditions, while heat transport is treated as developing. The problem is governed by 2-D momentum, 2-D induction, and 3-D energy equations in terms of the flow velocity (U), induced magnetic field (B_x) and temperature (T):

$$\frac{\partial}{\partial z}\left[\nu\frac{\partial U}{\partial z}\right]+\frac{\partial}{\partial y}\left[\nu\frac{\partial U}{\partial y}\right]-\frac{1}{\rho}\frac{dP}{d\mathrm{x}}+\frac{B_z^0}{\rho\mu}\frac{\partial B_x}{\partial z}=0; \quad (5)$$

$$\frac{1}{\mu}\frac{\partial}{\partial z}\left(\frac{1}{\sigma_z}\frac{\partial B_x}{\partial z}\right)+\frac{1}{\mu}\frac{\partial}{\partial y}\left(\frac{1}{\sigma_y}\frac{\partial B_x}{\partial y}\right)+B_z^0\frac{\partial U}{\partial z}=0; \quad (6)$$

$$\rho C_p U\frac{\partial T}{\partial x}=\frac{\partial}{\partial x}\left(k_x\frac{\partial T}{\partial x}\right)+\frac{\partial}{\partial y}\left(k_y\frac{\partial T}{\partial y}\right)+\frac{\partial}{\partial z}\left(k_z\frac{\partial T}{\partial z}\right)+q'''. \quad (7)$$

The coordinates *x*, *y* and *z* denote the poloidal, radial, and toroidal directions. The *x*-axis coincides with the channel axis. The coordinate origin is located in the bottom plane, at the flow inlet. Equation (5) is formulated for the PbLi only, while the other equations are written over the whole domain, including the FCI, ferritic wall, gap, and the bulk flow. The source term q^m stands for volumetric heating and is calculated separately using a neutronics code. B_z^0 denotes the applied (toroidal) magnetic field, which is in the reference flow is 4 T. The equations are solved with a finite-difference numerical code [60]. The code has specially been designed for channels with a "sandwich" structure of several materials with different physical properties. The code includes a finite-volume formulation, automatically generated Hartmann number sensitive meshes, and effective convergence acceleration technique. In the present calculations, the Hartmann number is 15,900. Other parameters used in the calculations are summarized in Table 2.

Results are presented for the blanket flow with the FCI without pressure equalization openings. The physical properties of the silicon carbide composite are not defined very well yet and can possibly be tailored to meet specific needs [61]. The computations were performed in a parametric form for σ_{SiC}=5-500 S/m and k_{SiC}=2-20 W/m-K. Figure 21 demonstrates the induced magnetic field distribution over the channel cross section (which is essentially a stream function for electric current). Electric currents generated in the bulk flow leave the internal domain through one of the FCI side walls and return back through the opposite wall. When interacting with the toroidal magnetic field, the induced currents create Lorentz force, which is responsible for special "M-type" velocity profiles (Fig. 21b). In all figures, the velocity is scaled by the mean flow velocity of the bulk flow U_0. The high velocity jets near the side walls reduce strongly as electrical conductivity of the SiC composite decreases (Fig. 22). However, even at σ_{SiC} =5 S/m, the jets do not fully disappear, indicating that electrical

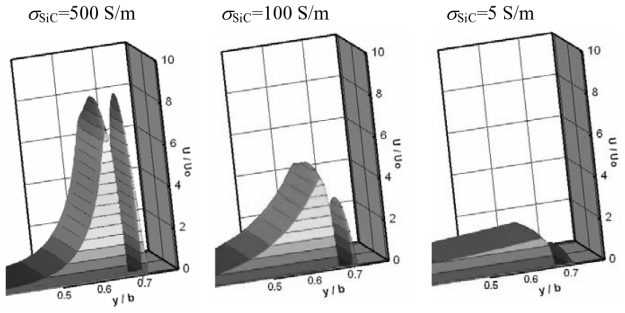

Fig. 22. Effect of the Electrical Conductivity of the SiC Composite on the Velocity Profile in the Bulk and in the Gap

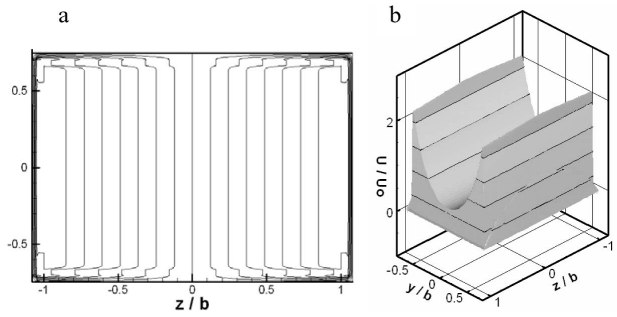

Fig. 21. Induced Magnetic Field (a) and Velocity Profile (b) in a Fully Developed Flow in the front Channel of the Reference DCLL Blanket at *Ha*=15,900, σ_{SiC}=20 S/m

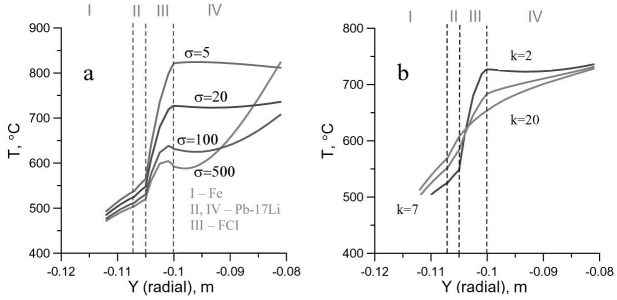

Fig. 23. Radial Temperature Variations in the Vicinity of the front wall at the Flow Exit Calculated at k_{SiC} = 2 W/m-K (a); σ_{SiC} = 20 S/m (b).

Table 2. Typical Blanket Channel Parameters

Poloidal length, *L*: 2 m	Ferritic wall thickness: 0.005 m
Toroidal width, *2b*: 0.3 m	PES width: 0.005 m
Radial depth, *2a* : 0.2 m	Magnetic field (outboard), B_z^0 : 4 T
FCI thickness: 0.005 m	Pb-17Li flow velocity, U_0 : 0.06 m/s
Gap width: 0.002 m	Inlet Pb-17Li temperature: 460°C

insulation is not perfect. Such a velocity profile has a strong effect on heat transfer.

Figure 23 shows the effect of σ_{SiC} and k_{SiC} on the radial temperature distribution at the channel top in a narrow region facing the first wall. The effect of k_{SiC} is obviously thermal insulation of the bulk flow region from the helium flows. The influence of σ_{SiC} is not so simple, since its variations result in significant changes of heat transfer through modifications of the liquid metal flows. Reduction of σ_{SiC} causes bigger temperature difference across the FCI, and hence higher thermal stresses. It also leads to higher interface temperatures between the ferritic wall and liquid metal. At the same time, reduction of σ_{SiC} is desirable because of smaller pressure losses. As a result, reduction of σ_{SiC} may lead to ambiguous consequences for the blanket performance.

With these numerical simulations, basic characteristics of MHD flow and heat transfer in the front poloidal channel of the reference DCLL blanket were studied. Under the particular conditions used in the analysis, parameters of the SiC_f/SiC FCI have been identified that result in low MHD pressure drop and reasonable heat leakage from the breeder into the helium flows. The results show that the MHD pressure drop can be reduced by 400 times compared to the case without insulation, if electrical conductivity of a silicon carbide composite is 5 $(\Omega m)^{-1}$. This conclusion, however, does not apply to liquid metal flows in other sections of the blanket module, such as manifolds, bends, contractions, expansions, *etc*., where the MHD pressure drop is mostly associated with the axial currents, which cannot be eliminated by insulating the channel walls. Special considerations are required for the entry effects over the inlet flow section, where the flow is not in the fully developed state, and for flows around a pressure equalization opening. These flows and their effect on heat and tritium transport will be a subject of a special analysis in the near future. It has been observed that if the thermal conductivity of SiC_f/SiC is 2 W/m-K or lower, the FCI acts as an ideal thermal insulator. However, these values of thermal and electrical conductivities are not universal and should be corrected if the design parameters are different from those considered in the present study. In addition, some heat leakage will likely occur in the return channels, where the temperature is above average. More improvements should be included in the future for better estimation of these important blanket performance parameters. Particularly, effects of natural convection and two-dimensional turbulence should be assessed and corresponding modifications of the present model made as necessary. More complete modeling will need to be done to include effects of electrical connection between flows in neighboring channels, which are not negligible, since the FCI is not a perfect insulator as shown in the present study. These modeling efforts should be accompanied with a broad materials program to develop fabrication techniques for the silicon carbide inserts and characterize their properties.

4. SUMMARY AND FUTURE DIRECTIONS

Research progress in the APEX project (1998-2003) and the US ITER TBM activities (2003-present) has been reviewed, with special emphasis placed on describing results in specific technical areas including liquid breeder magnetohydrodynamics, ceramic pebble bed thermomechanics, and tritium fuel cycle modeling.

A core focus of the APEX study was on new liquid wall concepts, where the various liquid wall configurations and modeling of flows of working liquids were discussed. Liquid metal walls, especially low vapor pressure liquid metals like tin, exhibit high surface temperature capabilities allowing large temperature windows and high outlet temperature coolants. Liquid lithium may be more desirable from a plasma physics perspective due to hydrogen and impurity gettering, but its temperature window for a power reactor application is more limited. Research into developing 3D MHD free surface simulations tools (HIMAG) is continuing, as MHD effects in liquid metals were identified as the key feasibility issue. This work is currently directed at geometries, phenomena, and parameter ranges typical of the NSTX plasma device in Princeton where the deployment of a liquid lithium divertor for particle control is being considered. APEX also re-considered the utilization of molten salts, specifically FLiBe and FLiNaBe as fusion reactor coolants. Effects of free surfaces on turbulent heat transfer were discussed at length, and it was noted that research effort on MHD effects on molten salt stimulant heat transfer and FLiBe chemistry control is continuing as part of the US-Japan JUPITER-II program.

The US ITER TBM program concentrates mostly on a conventional blanket design and R&D. A special emphasis was given to thermofluid issues as one of the most important components of any liquid blanket concept, and specifically for the DCLL concept being developed in the US. Current progress on selective R&D of closed channel blanket flows has been shown through modeling results. In addition, the HIMAG code discussed above for 3D free surface flows is being benchmarked for closed channel flows at high Hartmann number with multiple materials so that it can potentially be used together with other UCLA research codes for evaluating the effect of various phenomena and blanket elements including complex geometry FCIs, bends, manifolds, natural convection, *etc*. on the DCLL feasibility and performance.

Modeling and experimental investigation of the issues related to the development of solid breeder blankets has also been described. Particular focus in this case has been on the long-time thermomechanical behavior of packed pebble beds of ceramic breeder materials in typical solid breeder blanket designs. Future plans include further experiments with low mass test articles with local active cooling

that will allow to reproduce thermal cycles that are more representative of fusion energy power plant operation, as well as controlled thermal gradients across the pebble bed. Different combinations of structural, cladding and breeding materials as well as test article geometries will be tested. The cumulative effect of the plastic deformation of the bed will be studied to investigate the possible formation of gaps between the pebbles and the surrounding structural material. Continued model development and benchmarking is a vital part of this effort for developing a usable predictive capability for bed behavior.

Acknowledgements

The authors would like to acknowledge the support of the Department of Energy and the participation of the many researchers involved in APEX, US ITER TBM and the other fusion technology program in the US over the past decade.

REFERENCES

[1] M. Abdou, "ITER Test Program: Key Technical Aspects," *Fusion Technology* **19**, 1439-1451: (1991).

[2] M. Abdou, "A Volumetric Neutron Source for Fusion Nuclear Technology Testing and Development," *Fusion Eng. Des*. **27**, 111-153 (1995).

[3] M. Sawan, M. Abdou, "Physics and technology conditions for attaining tritium self-sufficiency for the D-T fuel cycle", presented at the 7th International Symposium on Fusion Nuclear Technology, May 22-27 2005, Tokyo, Japan and to be published in *Fusion Eng. Des*. (2005).

[4] M. Sawan, "Geometrical, Spectral and Temporal Differences between ICF and MCF Reactors and Their Impact on Blanket Nuclear Parameters," *Fusion Technol*. **10**, 1483-1488 (1986).

[5] M. Youssef and M. Abdou, "Uncertainties in Prediction of Tritium Breeding in Candidate Blanket Designs Due to Present Uncertainties in Nuclear Data Base," *Fusion Technol.* **9**, 286-306 (1986).

[6] M. Sawan et al., "Neutronics Assessment of Molten Salt Breeding Blanket Design Options," *Fusion Sci. Technol*. **47**, 510-517 (2005).

[7] L.A. El-Guebaly and the ARIES Team, "Three-Dimensional Neutronics Study for ARIES-ST Power Plant," *Fusion Technol*. **34**, 1084-1088 (1998).

[8] M. Youssef, M. Sawan, A. Ying, "Nuclear analysis of two "look-alike" helium-cooled pebble bed test blanket sub-modules proposed by the US for testing in ITER", presented at the 7th International Symposium on Fusion Nuclear Technology, May 22-27 2005, Tokyo, Japan and to be published in *Fusion Eng. Des*. (2005).

[9] M. Sawan and M. Youssef, "Three-Dimensional Neutronics Assessment of Dual Coolant Molten Salt Blankets with Comparison to One-Dimensional Results," presented at the 7th International Symposium on Fusion Nuclear Technology, May 22-27 2005, Tokyo, Japan and to be published in *Fusion Eng. Des* (2005).

[10] L. El-Guebaly and the ARIES Team, "Potential Coatings for Li/V System: Nuclear Performance and Design Issues," presented at the 7th International Symposium on Fusion Nuclear Technology, May 22-27 2005, Tokyo, Japan and to be published in *Fusion Eng. Des* (2005).

[11] M. Abdou, E. Vold, C. Gung, M. Youssef and K. Shin, "Deuterium-Tritium Fuel Self-Sufficiency in Fusion Reactors", *Fusion Technol*. **9**, 250-285 (1986).

[12] W. Kuan and M. Abdou, "A New Approach for Assessing the Required Tritium Breeding Ratio and Startup Inventory in Future Fusion Reactors", *Fusion Technol*. **35**, 309-353 (1999).

[13] M. Abdou and the APEX Team, "Exploring Novel High Power Density Concepts for Attractive Fusion Systems", *Fusion Eng. Des*. **45**, 145-167 (1999).

[14] M.A. Abdou and the APEX Team, "On the exploration of innovative concepts for fusion chamber technology," *Fusion Eng. Des*. **54**, 181-247 (2001).

[15] C.P.C. Wong, S. Malang, S. Nishio, R. Raffray, A. Sagara, "Advanced high performance solid wall blanket concepts," *Fusion Eng. Des*. **61-62**, 283-293 (2002).

[16] C.P.C. Wong, S. Malang, M. Sawan, I. Sviatoslavsky, E. Mogahed, S. Smolentsev, S. Majumdar, B. Merrill, R. Mattas, M. Friend *et al*. "Molten salt self-cooled solid first wall and blanket design based on advanced ferritic steel", *Fusion Eng. Des*. **72**, 245-275 (2004).

[17] L.E. Zakharov, "Magnetic propulsion of intense lithium streams in a tokomak magnetic field," *Phys. Rev. Lett*. **90**, 045001/1-4 (2003) .

[18] F. Najmabadi and the ARIES Team, "Overview of ARIES -RS tokamak fusion power plant," *Fusion Eng. Des.* **41**, 365 -370 (1998).

[19] A.Y. Ying, M.A. Abdou, N. Morley, T. Sketchley, R. Woolley, J. Burris, R. Kaita, P. Fogarty, H. Huang, X. Lao et al., "Exploratory studies of flowing liquid metal divertor options for fusion-relevant magnetic fields in the MTOR facility," *Fusion Eng. Des*. **72**, 35-62 (2004) .

[20] K. Gulec, M. Abdou, R. W. Moir, N. B. Morley, A. Y. Ying, "Novel liquid blanket configurations and their hydrodynamic analyses for innovative confinement concepts," *Fusion Eng. Des*. **49-50**, 567-576 (2000).

[21] R.E. Nygren, T.D. Rognlien, M.E. Rensink, S.Y. Smolentsev, M.Z. Youssef, M.E. Sawan, B.J. Merrill, C. Eberle, P.J. Fogarty, B.E. Nelson *et al*., "A fusion reactor design with a liquid first wall and divertor," *Fusion Eng. Des*. **72**, 181-221 (2004).

[22] T.D. Rognlien and M.E. Rensink, "Edge-plasma properties in liquid-wall environments," 8th Int. Workshop on Edge Plasma Theory in Fusion Devices, Helsinki, Finland, (Sep. 2001).

[23] N.B. Morley, S. Smolentsev and D. Gao, "Modeling infinite /axisymmetric liquid metal magnetohydrodynamic free surface flows," *Fusion Eng. Des*. **63-64**, 343-351 (2002).

[24] J.M. McDonald, R.E. Nygren, T.J. Lutz, T.J. Tanaka, M.A. Ulrickson, T.J. Boyle, K.P. Troncosa, "Measurement of the melting point temperature of several lithium-sodium-beryllium fluoride salt (flinabe) mixtures." *Fusion Sci. Technol*., **47**, 554-8 (2005).

[25] N.B. Morley, M.A. Abdou, M. Anderson, P. Calderoni, R.J. Kurtz, R. Nygren, R. Raffray, M. Sawan, P. Sharpe, S. Smolentsev, S. Willms, A.Y. Ying, "Overview of Fusion Nuclear Technology in the US," presented at the 7th International Symposium on Fusion Nuclear Technology, May 22-27

2005, Tokyo, Japan and to be published in *Fusion Eng. Des*. (2005).
[26] C.P.C. Wong, S. Malang, M.Sawan, M. Dagher, S.Smolentsev, *et al*., "An overview of dual coolant Pb-17Li breeder first wall and blanket concept development for the US ITER-TBM design," presented at the 7th International Symposium on Fusion Nuclear Technology, May 22-27 2005, Tokyo, Japan and to be published in *Fusion Eng. Des*. (2005).
[27] P.F. Peterson, "Multiple-reheat Brayton cycles for nuclear power conversion with molten coolants," *Nucl. Tech*. **144**, 279-288 (2003).
[28] J.N. Brooks, J.P. Allain, R. Bastasz, R. Doerner, T. Evans, A. Hassanein, R. Kaita, S. Luckhardt, R. Maingi, R. Majeski, N.B. Morley, N. Narula, T. Rognlien,, D. Ruzic, R. Stubbers, M. Ulrickson, C.P.C. Wong, A. Ying, "Overview of the ALPS Program," *Fusion Sci. Technol*. **47**, 669-677 (2005).
[29] P.V. Dankwerts, "Significance of liquid-film coefficients in gas absorption," *Ind. Eng. Chem*. **43**, 1460-1467 (1951).
[30] S. Smolentsev, N. Morley, B. Freeze, R. Miraghaie, J.-C. Nave, S. Banerjee, A. Ying and M. Abdou, "Thermofluid modeling and experiments for free surface flows of low-conductivity fluid in fusion systems," *Fusion Eng. Des*.. **72**, 63-81 (2004).
[31] S. Smolentsev, M. Abdou, N. Morley, A. Ying, T. Kunugi, "Application of the K-e model to open channel flows in a magnetic field," *Int. J. of Eng. Sci*. **40**, 693-711 (2002).
[32] B. Freeze, S. Smolentsev, N. Morley, M. Abdou, "Characterization of the effect of Froude number on surface waves and heat transfer in inclined turbulent open channel water flows," *Int. J. Heat Mass Trans*. **46**, 3765-3775 (2003).
[33] S. Satake, T. Kunugi, S. Smolentsev, "Advances in direct numerical simulation for MHD modeling of free surface flows," *Fusion Eng. Des*. **61-62**, 95-102 (2002).
[34] S. Smolentsev, R. Miraghaie, "Study of a free surface in open-channel water flows in the regime from 'weak' to 'strong' turbulence," *Int. J. Multiphase Flow*, **31**, 921-939 (2005).
[35] N.B. Morley, J. Burris, "The MTOR LM-MHD flow facility, and preliminary experimental investigation of thin layer, liquid metal flow in a 1/R toroidal magnetic field," *Fusion Sci. Technol*. **44**, 74-78 (2003) .
[36] N.B. Morley, S. Smolentsev, R. Munipalli, M.-J. Ni, D. Gao and M. Abdou, "Progress on the modeling of liquid metal, free surface, MHD flows for fusion liquid walls," *Fusion Eng. Des*. **72**, 3-34 (2004).
[37] H. L. Huang, A. Ying and M. A. Abdou, "3D MHD free surface fluid flow simulation based on magnetic-field induction equations," *Fusion Eng. Des*. **63-64**, 361-368 (2002).
[38] S. Smolentsev, M. Abdou, T.Kunugi, N.B. Morley, S.Satake and A. Ying, "Modeling of liquid walls in APEX study," *Int. J. Appl. Electromag. Mech*. **13**, 373-379 (2001/2002).
[39] S. Smolentsev, M. Abdou, "Open-surface MHD flow over a curved wall in the 3-D thin-shear-layer approximation," *Appl. Math. Model*. **29**, 215-234 (2005).
[40] D. Gao, N.B. Morley, V. Dhir, "Numerical simulation of wavy falling film flows using VOF method," *J. Comp. Phys*. **192**, 624-642 (2003).
[41] D. Gao, N.B. Morley, "Equilibrium and initial linear stability analysis of liquid metal falling film flows in a varying spanwise magnetic field," *Magnetohydrodynamics*, **38**, 359-375 (2002).
[42] R. Munipalli et al. "Development of a 3-D incompressible free surface MHD computational environment for arbitrary geometries: HIMAG." DOE SBIR Phase-II Final Report (Jun 2003).
[43] J.H. Fokkens, "Thermo-Mechanical Finite Element Analyses for the HCPB In-Pile Test Element," NRG, Petten, 21477/02.50560/P (Jun 2003).
[44] D. Hofer, M. Kamlah, S. Hermsmeyer, "Revision of Drucker-Prager cap creep modelling of pebble beds in fusion blankets," presented at CBBI-11, Tokyo (Dec. 2003).
[45] A. Ying, H. Huang and M. Abdou, "Numerical simulation of ceramic breeder thermal creep behavior," *J. Nucl. Mat*. **307-311**, 827-831 (2002).
[46] A.Y. Ying, T. Yokomine, A. Shimizu, M. Abdou, A. Kohyama, "Impact of Material System Thermomechanics and Thermofluid Performance on He-Cooled Ceramic Breeder Blanket Designs with SiCf/SiC," *J. Nucl. Mat*. **329-333PB**, 1605-1609 (2004).
[47] M.C. Billone, Y.Y. Liu, R.B. Poeppel, J.L. Routbort, K.C. Goretta, D.S. Kupperman, "Elastic and Creep Properties of Li2O," *J. Nucl. Mat*. **141-143**, 282-288, (1986).
[48] L. Bühler, "Continuum models for pebble beds in fusion blankets," FZKA 6561, (2002).
[49] F. Parhami, R.M. McMeeking, A.C.F. Cooks, Z. Suo, "A model for the sintering and coarsening of rows of spherical particles," *Mechanics of Materials*, **31**, 43-61 (1999).
[50] MSC MARC, MSC Software Corporation, Los Angeles (Mar 2000).
[51] J. Reimann, E. Arbogast, S. Muller, K. Thomauske, "Thermomechanical behavior of ceramic breeder pebble beds," Proceedings of CBBI-7, 5.1-5.10 (Sep 1988).
[52] J. Reimann and G. Wörmer, "Thermal creep of Li4SiO4 pebble beds," *Fusion Eng. Des*. **58-59**, 647-651 (2001).
[53] A. Ying, M. Abdou, P. Calderoni, S. Sharafat, M. Youssef, Z. An, A. Abou-Sena, E. Kim, S. Reyes, S. Willms, R. Kurtz, "Solid Breeder Test Blanket Module Design and Analysis," presented at the 7th International Symposium on Fusion Nuclear Technology, May 22-27 2005, Tokyo, Japan and to be published in *Fusion Eng. Des*. (2005).
[54] P. Calderoni, A. Ying, T. Sketchley, M.A. Abdou, "Experimental study of the interaction of ceramic breeder pebble beds with structural materials under thermo-mechanical loads," presented at the 7th International Symposium on Fusion Nuclear Technology, May 22-27 2005, Tokyo, Japan and to be published in *Fusion Eng. Des*. (2005).
[55] M.S. Tillack, S. Malang, High Performance PbLi blanket, Proc.17th IEE/NPSS Symposium on Fusion Engineering, Vol. 2, 1000-1004, San Diego, California (Oct 1997).
[56] D.K. Sze, M. Tillack et al., "Blanket system selection for ARIES ST," *Fusion Eng. Des*. **48**, 371-378 (2000).
[57] P. Norajitra, L. Buhler, U. Fischer, K. Kleefedt, S. Malang et al., "The EU advanced dual coolant blanket concept using SiCf/SiC flow channel inserts as electrical and thermal insulators," *Fusion Eng. Des*. **58-59**, 629-634 (2001).
[58] S.Smolentsev, M. Abdou, N.B. Morley, M. Sawan, S. Malang, C. Wong, "Numerical analysis of MHD flow and heat transfer in a poloidal channel of the DCLL blanket with a SiC_f /SiC flow channel insert," presented at the 7th International Symposium on Fusion Nuclear Technology, May 22-27 2005, Tokyo, Japan and to appear *Fusion Eng. Des*. (2005).
[59] S. Smolentsev, M. Abdou, "Effect of a magnetic field on

heat transfer in liquid metal channel flows under conditions of a fusion power reactor," HEFAT 2005, 4th International Conference on Heat Transfer, Fluid Mechanics and Thermodynamics, Cairo, Egypt (Sep 2005).

[60] S. Smolentsev, N.B. Morley, M. Abdou, "Code development for analysis of MHD pressure drop reduction in a liquid metal blanket using insulation technique based on a fully developed flow model," *Fusion Eng. Des*. **73**, 83-93 (2005).

[61] A.R. Raffray *et al*., "Design and material issues for high performance SiC_f/SiC-based fusion power cores," *Fusion Eng. Des*. **55**, 55-95 (2001).